Aircraft Longitudinal Pitch Control System

Modeling, Classical and State-Space Control Design, Actuator-Constrained Simulation, and Robustness Analysis

Final Engineering Project Report

Prepared by **Mohana Lotfi**

Mechanical Engineering
Concordia University
Montréal, Québec, Canada

August 2026

Abstract

This project develops and evaluates a longitudinal aircraft pitch-control system using a documented Boeing 747 linear small-perturbation model at a specified cruise operating condition. The study progresses from open-loop flight-dynamics characterization through classical feedback design, actuator-constrained simulation, robustness assessment, and advanced full-state control. The aircraft model was reconstructed and validated in MATLAB, then independently implemented in Simulink to verify numerical consistency between the two environments. Open-loop analysis identified stable short-period and lightly damped phugoid modes, with the latter producing extremely slow natural settling and demonstrating the need for feedback control. Proportional, proportional-integral, and filtered proportional-integral-derivative controllers were developed and quantitatively compared before introducing a documented Boeing 747-100/200 elevator-actuator model with finite dynamics, travel limits, and a 37°/s rate limit. Actuator analysis showed that an apparently satisfactory ideal-actuator design could demand approximately 148°/s of elevator motion, motivating actuator-aware PID redesign. The resulting final PID achieved 15.881% nominal overshoot and a 27.074 s settling time while satisfying the adopted actuator constraints. Sensitivity studies showed that reduced elevator effectiveness was the dominant tested uncertainty and caused the PID to exceed the project settling-time target while remaining stable and physically feasible. LQR and LQI full-state controllers were subsequently investigated, and a structured multi-case LQI tuning study produced the strongest overall simulated performance. The final tuned LQI achieved 0.6336% nominal overshoot, 5.5741 s settling time, and substantially lower actuator-rate demand while also maintaining strong performance under reduced elevator effectiveness and the tested control-channel disturbance. Final frozen-configuration validation and numerical consistency audits confirmed the reproducibility of the reported results. The study demonstrates how progressively incorporating actuator realism, uncertainty, disturbance rejection, and implementation constraints can materially influence aircraft control-system design decisions.

Table of Contents

List of Figures

List of Tables

1. Introduction and Objectives

1.1 Background and Motivation

Aircraft longitudinal control governs motion in the vertical plane and is particularly concerned with the relationship between elevator deflection, pitch rate, and aircraft pitch attitude. A pitch-control system must provide accurate command tracking while maintaining stable aircraft motion and avoiding excessive control-surface activity.

Although an aircraft may be naturally stable at a particular flight condition, open-loop stability alone does not guarantee satisfactory command-following performance. Lightly damped longitudinal modes can produce long settling times and significant pitch excursions following control inputs or external disturbances. Feedback control is therefore used to improve transient response, tracking accuracy, disturbance rejection, and overall dynamic behavior.

This project investigates longitudinal pitch control using a documented Boeing 747 small-perturbation model. The analysis is performed using MATLAB and Simulink and progresses from open-loop aircraft characterization to classical feedback control, actuator-constrained simulation, robustness analysis, and advanced full-state feedback control.

1.2 Project Objective

The primary objective of this project is to develop, simulate, and evaluate a longitudinal aircraft pitch-control system in which elevator deflection is used to regulate aircraft pitch angle.

The controlled output is the pitch-angle perturbation, θ ,while the primary control input is elevator deflection, δ_e . Positive pitch angle represents a nose-up aircraft attitude. The elevator sign convention follows the documented Boeing 747 model used in the analysis.

The project is intended to evaluate not only whether a controller can track a commanded pitch angle, but also whether the resulting response is dynamically stable, quantitatively satisfactory, and compatible with the adopted actuator capabilities.

1.3 Aircraft Modeling Scope

The aircraft is represented using a linear longitudinal small-perturbation model about a specified trimmed cruise condition.

The longitudinal state vector used throughout the project is $x = [u \quad w \quad q \quad \theta]^T$, where:

- (u) is the forward-velocity perturbation,
- (w) is the vertical body-axis velocity perturbation,
- (q) is the pitch-rate perturbation,
- (θ) is the pitch-angle perturbation.

The aircraft dynamics are expressed in state-space form as $\dot{x} = Ax + B\delta_e$, with pitch angle selected as the primary controlled output.

The model represents rigid-body longitudinal motion near one specified trimmed flight condition. Lateral-directional motion, structural flexibility, aeroelastic effects, stall behavior, large-angle nonlinear aerodynamics, and physical hardware implementation are outside the scope of the present study.

Consequently, the results should be interpreted as control-system performance for small perturbations near the selected operating condition rather than as a complete representation of the aircraft flight envelope.

1.4 Control-System Development Objectives

The controller-development process was structured to increase both control sophistication and physical realism progressively.

The study includes:

1. characterization of the natural open-loop longitudinal dynamics;
2. development and comparison of proportional, proportional-integral, and proportional-integral-derivative control;
3. MATLAB and Simulink cross-validation;
4. introduction of realistic elevator-actuator dynamics, travel limits, and rate limits;
5. disturbance-rejection assessment;
6. sensitivity and robustness analysis under model perturbations;
7. development of LQR and LQI full-state feedback control;
8. final comparison and validation of the classical PID and advanced LQI designs.

This progression allows each design decision to be evaluated against a validated baseline rather than introducing all controller and actuator effects simultaneously.

1.5 Performance and Engineering Evaluation Criteria

Controller performance is evaluated quantitatively rather than solely through visual inspection of response plots.

The primary performance measures are:

- steady-state pitch tracking error,
- percentage overshoot,
- peak pitch response,
- peak time,
- 2% settling time,
- disturbance-induced pitch deviation,
- disturbance recovery time,

- elevator deflection,
- elevator deflection rate,
- closed-loop stability,
- sensitivity to changes in aircraft-model parameters.

For the main $(5°)$ pitch-command studies, project-level screening targets of $M_p \leq 20\%$ And $t_s \leq 30$ s were adopted for controller comparison. These values are engineering design targets used within this project and are not presented as aircraft certification requirements.

Actuator feasibility is assessed using the adopted elevator travel and rate constraints introduced later in the report.

1.6 Computational Approach

MATLAB is used for state-space implementation, eigenvalue and pole analysis, time-domain simulation, controller design, numerical parameter studies, and quantitative performance calculations.

Simulink is used to construct explicit closed-loop control architectures and to introduce actuator dynamics and nonlinear control-surface constraints.

Independent MATLAB–Simulink comparisons are performed at several stages to verify that the block-diagram implementations reproduce the corresponding analytical or state-space models.

Validated aircraft and controller configurations are stored separately from the analysis scripts so that later simulations use consistent baseline data and final controller parameters.

1.7 Project Outcome Sought

The purpose of the project is not simply to obtain the fastest possible pitch response. The final controller must represent an engineering balance between:

$$\left[\boxed{\text{tracking performance} + \text{stability} + \text{disturbance rejection} + \text{robustness} + \text{actuator feasibility}}\right]$$

The final design is therefore selected using multiple quantitative criteria and is validated under nominal operation, actuator constraints, external disturbance, and reduced control effectiveness.

2. Aircraft Model and Assumptions

2.1 Baseline Aircraft Model

A documented Boeing 747 longitudinal dynamics model was selected as the baseline aircraft plant for the control-system study.

The model represents steady level cruise at approximately $M = 0.8$ and an altitude of $h = 40{,}000\ ft$. The corresponding trim forward speed used in the MATLAB implementation is approximately $U_0 = 235.9\ \text{m}/s$. The aircraft model is a linear small-perturbation representation developed about this specific trim condition. It therefore describes the local longitudinal dynamics of the aircraft rather than its behavior across the complete flight envelope.

The model was implemented from documented aircraft properties and dimensional stability and control derivatives rather than from arbitrarily selected coefficients.

2.2 Longitudinal State Definition

The longitudinal state vector is $\mathbf{x} = \begin{bmatrix} u \\ w \\ q \\ \theta \end{bmatrix}$, where $u = \text{forward-velocity perturbation (m/s)}$, $w = \text{vertical body-axis velocity perturbation (m/s)}$, $q = \text{pitch-rate perturbation (rad/s)}$, and $\theta = pitch - angle\ perturbation\ (rad)$.

The complete documented aircraft model contains both elevator and thrust perturbation inputs.

For the present pitch-control study, elevator deflection δ_e was isolated as the control input. Pitch angle θ was selected as the primary controlled output.

2.3 Elevator Sign Convention

The source aircraft model defines positive elevator deflection as **elevator-down motion**.

The elevator-to-pitch plant has a negative steady-state gain. Therefore, under this convention, a negative elevator deflection produces a positive steady-state pitch-angle perturbation.

Consequently, a positive nose-up pitch command generally requires a negative physical elevator command.

This sign convention is retained consistently throughout the classical and full-state feedback controller designs.

2.4 State-Space Representation

The longitudinal dynamics are represented by $\dot{x} = Ax + B_e\delta_e$ and $\theta = C_\theta x + D_\theta \delta_e$. Using the state ordering $[u,\ w,\ q,\ \theta]^T$, the reconstructed state matrix, rounded for presentation, is approximately:

$$A = \begin{bmatrix} -0.0069 & 0.0139 & 0 & -9.81 \\ -0.0905 & -0.3149 & 235.8928 & 0 \\ 0.0004 & -0.0034 & -0.4282 & 0 \\ 0 & 0 & 1 & 0 \end{bmatrix}$$

The final row represents the kinematic relationship $\dot{\theta} = q$.

The elevator-input vector is approximately $B_e = \begin{bmatrix} -5.73 \times 10^{-5} \\ -5.508 \\ -1.157 \\ 0 \end{bmatrix}$.

The final zero entry indicates that elevator deflection does not instantaneously change pitch angle. Instead, elevator motion changes the aircraft aerodynamic forces and pitching moment, which modify the dynamic states and ultimately change pitch attitude.

Pitch angle is extracted using $C_\theta = [0 \quad 0 \quad 0 \quad 1]$, with $D_\theta = 0$.

Although only pitch angle is selected as the primary external output for the classical control analysis, the complete four-state model is retained internally. This becomes important later when full-state LQI feedback is introduced.

2.5 Model Reconstruction

Rather than directly copying the published numerical state-space matrix, the aircraft matrices were reconstructed in MATLAB from the documented dimensional stability and control derivatives.

The complete input structure was reconstructed first before the elevator channel was isolated for pitch-control development.

This approach improved traceability because the implemented state-space model could be checked against:

1. the source aircraft parameters,
2. the dimensional stability derivatives,
3. the longitudinal state equations,
4. the published numerical state-space model.

The resulting plant contains 4 states, 1 elevator control input, and 1 $primary\ pitch - angle\ output$.

Programmatic matrix-dimension checks were included in MATLAB to prevent accidental modification of the model structure.

The automated dimension validation returned $[\boxed{\text{PASS}}]$.

2.6 Numerical Validation of the Aircraft Model

The independently reconstructed state matrix was compared with the published numerical model.

Only small discrepancies were observed, attributable primarily to the limited decimal precision of the published comparison coefficients.

The maximum absolute state-matrix entry difference was approximately 4.37×10^{-5}.

This agreement provides greater confidence in the implementation than directly copying the final state-space matrix because it confirms consistency between the underlying aircraft data and the resulting dynamic model.

The validated aircraft plant was subsequently frozen and used without modification throughout the remaining controller-development phases.

2.7 Frozen Baseline Model

Following reconstruction and validation, the final aircraft plant was saved as B747_longitudinal_baseline.mat.

This file contains the validated baseline aircraft model used by all subsequent MATLAB and Simulink analyses.

Freezing the baseline model prevents later controller-development scripts from unintentionally modifying or reconstructing the aircraft dynamics differently.

The project therefore separates $\left[\boxed{\text{validated aircraft plant}}\right]$ from $\left[\boxed{\text{controller design and simulation scripts}}.\right]$

This improves reproducibility and ensures that comparisons between different controller architectures use the same aircraft model.

2.8 Modeling Assumptions

The following assumptions apply to the baseline aircraft model:

- the aircraft is treated as a rigid body;
- motion is restricted to the longitudinal plane;
- the analysis is performed about a steady trimmed cruise condition;
- perturbations from trim are sufficiently small for linearization;
- lateral-directional dynamics are neglected;
- elevator deflection is treated as the primary pitch-control input;
- structural flexibility and aeroelastic effects are neglected;
- atmospheric and aircraft parameters correspond to the selected baseline operating condition.

The linear model should therefore not be interpreted as a complete high-fidelity Boeing 747 simulation.

2.9 Model Limitations

The state-space model is valid locally around the selected cruise trim condition.

The analysis does not explicitly represent:

- stall or separated-flow aerodynamics,
- large-angle maneuvers,
- large deviations in Mach number or altitude,
- nonlinear aerodynamic coefficients,
- lateral-directional coupling,

- structural flexibility,
- aeroelasticity,
- sensor dynamics or measurement noise,
- complete flight-control-computer implementation.

Later robustness studies perturb selected model characteristics to evaluate controller sensitivity, but these studies do not replace a full nonlinear flight-envelope model.

Accordingly, the results of this project should be interpreted as a comparative longitudinal flight-control design study around one documented operating condition.

3. Open-Loop Longitudinal Dynamics

3.1 Objective

Before introducing feedback control, the validated Boeing 747 longitudinal model was analyzed in open loop to establish its natural dynamic behavior.

The analysis focused on:

- open-loop stability,
- short-period and phugoid modes,
- response to a small elevator perturbation,
- steady-state elevator-to-pitch behavior,
- transient amplitude and settling,
- consistency between modal and time-domain predictions.

This open-loop characterization provides the baseline against which the closed-loop controllers are evaluated.

3.2 Open-Loop Poles and Stability

The eigenvalues of the longitudinal state matrix were calculated independently using the state matrix and the complete state-space model.

Both methods produced the pole pairs $\lambda_{1,2} - 0.3717 \pm 0.8869i$ and $\lambda_{3,4} - 0.0033 \pm 0.0672i$.

All four poles have negative real parts. Therefore, the linearized aircraft is asymptotically stable at the selected cruise operating condition.

However, the two pole pairs have substantially different time scales and damping characteristics.

3.3 Longitudinal Mode Identification

The faster pole pair $-0.3717 \pm 0.8869i$ was identified as the **short-period mode**. Its calculated characteristics were $\omega_n = 0.9617\ \mathrm{rad/s}$, $\zeta = 0.3865$, $T = 7.0842\ s$, with an approximate exponential decay time constant of

$\tau = 2.6903\ s$. The slower pole pair $-0.0033 \pm 0.0672i$ was identified as the **phugoid mode**. Its characteristics were $\omega_n = 0.0673\ \text{rad/s}, \zeta = 0.0489, T = 93.4971\ s$, and $\tau \approx 303.03\ s$.

The modal properties are summarized below.

Table 1. Open-Loop Longitudinal Mode Characteristics

Mode	Poles	$\omega_n$rad/s	ζ	Period (s)	Decay time constant (s)
Short period	$-0.3717 \pm 0.8869i$	0.9617	0.3865	7.0842	2.6903
Phugoid	$-0.0033 \pm 0.0672i$	0.0673	0.0489	93.4971	303.03

The short-period mode decays relatively quickly, whereas the phugoid mode is only weakly damped and persists for several minutes.

Thus, although the aircraft is mathematically stable, its long-period transient behavior is extremely slow.

3.4 Elevator-to-Pitch Open-Loop Test

A small elevator step of $\delta_e = -1°$ was applied to the aircraft.

Under the adopted sign convention, this represents a one-degree elevator-up perturbation.

A small input was intentionally used to remain consistent with the small-perturbation assumptions of the linearized aircraft model.

The elevator-to-pitch DC gain was $K_{DC} = -0.9230\ \text{rad/rad}$. The corresponding predicted steady-state pitch response is therefore $\theta_{ss}(-0.9230)(-1°) + 0.9230°$.

The response sign is physically consistent with the adopted model convention: elevator-up motion produces a positive nose-up pitch perturbation.

3.5 Open-Loop Time-Domain Response

The 400-second simulation exhibited a large, slowly decaying oscillatory pitch response.

The maximum pitch angle was $\theta_{\max} = 6.1432°$ at approximately $t = 22.60\ s$, while the first major negative excursion reached $\theta_{\min} = -3.5534°$ at approximately $t = 69.40\ s$.

The spacing between major long-period response peaks was consistent with the independently calculated phugoid period of approximately 93.5 s.

This agreement connects the eigenvalue-based modal analysis directly with the observed aircraft time response.

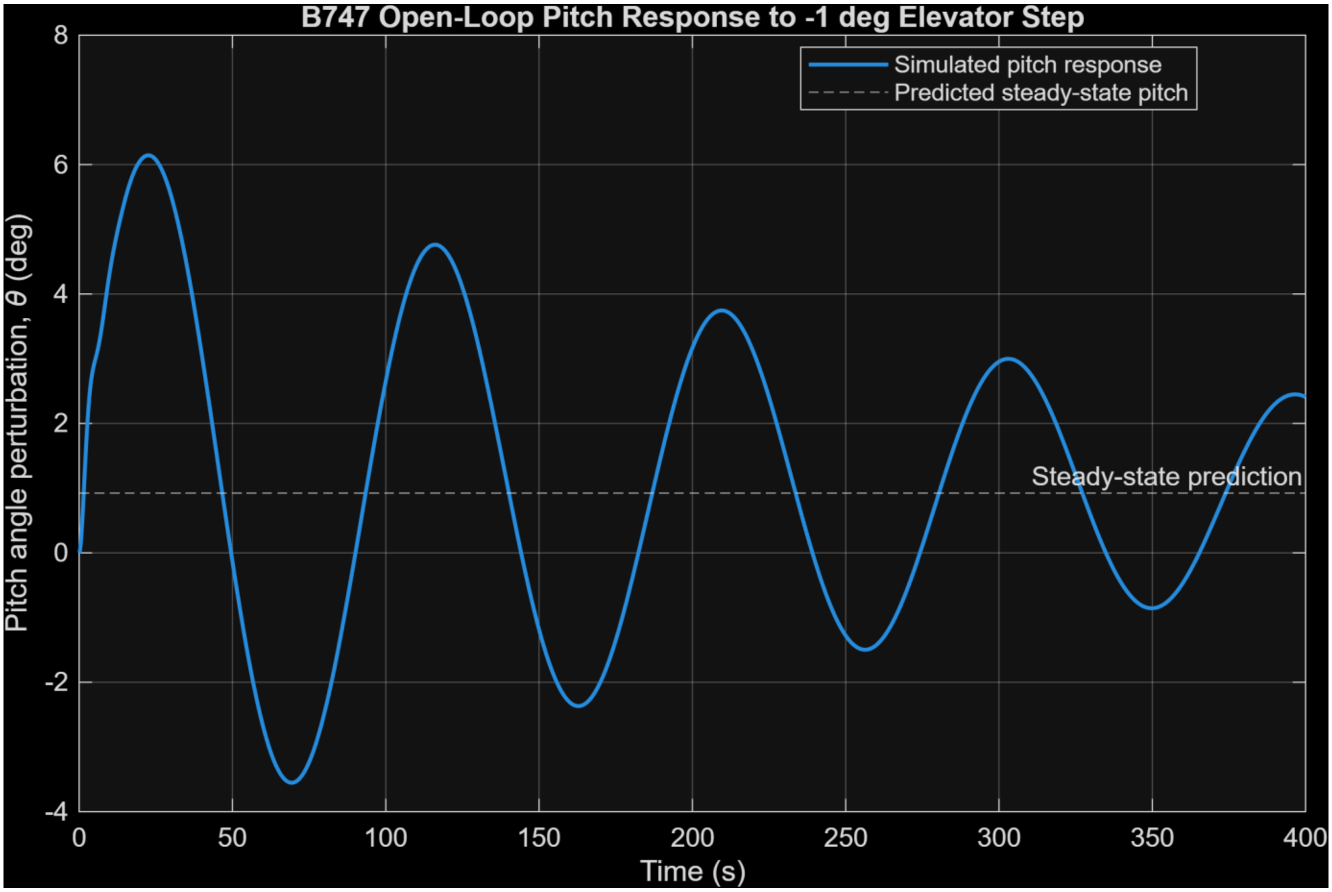

Figure 1. Open-loop Boeing 747 pitch-angle response to a -1° elevator step, showing the lightly damped long-period phugoid oscillation and the independently predicted steady-state pitch angle.

3.6 Open-Loop Settling Behavior

Using a 2% settling criterion around the independently predicted steady-state value, the calculated open-loop settling time was $t_s = 1712.41$ s or approximately 28.5 min.

Although this value initially appears unusually large, it is consistent with the very lightly damped phugoid mode.

The real component of the phugoid poles is approximately $\sigma = -0.0033\ \mathrm{s}^{-1}$, corresponding to a decay time constant of approximately $303\ s$.

An independent exponential-envelope estimate produced a settling time of the same order as the numerical simulation.

Therefore, the extremely long settling time is a physical consequence of the modeled phugoid dynamics rather than a numerical simulation error.

3.7 Long-Duration Steady-State Validation

A separate 2000-second simulation was performed to determine whether the oscillatory response eventually converged toward the independently calculated DC-gain prediction.

The predicted steady-state pitch angle was $0.9230°$, while the simulated response at 2000 seconds was approximately $0.9279°$.

The absolute difference was approximately $0.004922°$, corresponding to about 0.53% of the predicted steady-state value.

The small remaining difference is consistent with residual phugoid motion after several decay time constants.

This provides an independent confirmation of the steady-state gain calculation.

3.8 Open-Loop Validation Summary

The open-loop aircraft analysis was checked using several independent methods:

1. the eigenvalues of (A) and the poles of the state-space system agreed;
2. the calculated phugoid period agreed with the long-period oscillation observed in the simulated response;
3. the elevator-to-pitch DC gain independently predicted the steady-state pitch response;
4. the long-duration simulation approached the DC-gain prediction to within approximately 0.53%;
5. the unusually long settling time was independently consistent with the phugoid decay rate.

The agreement between these independent checks increases confidence that the open-loop behavior is a property of the implemented aircraft model rather than a numerical or software configuration error.

3.9 Engineering Interpretation

The baseline Boeing 747 model is open-loop stable at the selected cruise condition, but its natural response is not suitable for accurate or rapid pitch-command tracking.

The short-period mode is reasonably damped and decays comparatively quickly. In contrast, the phugoid mode has a damping ratio of only $\zeta \approx 0.049$, resulting in persistent long-period oscillation and extremely slow convergence.

Even a small $-1°$ elevator perturbation produces pitch excursions between approximately $-3.55°$ and $+6.14°$ during the initial response.

The open-loop aircraft therefore demonstrates an important control-design distinction: natural stability does not imply satisfactory control performance.

Feedback control is required to obtain substantially faster command tracking and improved transient behavior while maintaining realistic elevator demand.

4. Classical Pitch-Control Design

4.1 Control Objective

After establishing the open-loop longitudinal behavior, feedback control was introduced to track a commanded aircraft pitch angle.

The principal test command was $\theta_{cmd} = 5°$.

Three classical controller architectures were developed sequentially:

$$\boxed{\boxed{\mathrm{P} \rightarrow \mathrm{PI} \rightarrow \mathrm{PID}}}$$

The purpose of this progression was to identify the contribution of proportional, integral, and derivative feedback before introducing actuator nonlinearities later in the study.

Performance was evaluated using:

- steady-state tracking error,
- maximum pitch angle,
- percentage overshoot,
- 2% settling time,
- closed-loop stability,
- elevator demand.

At this stage, the elevator was treated as an ideal control input. Physical actuator travel and rate limitations are introduced separately in Section 6.

4.2 Feedback Sign Convention

The pitch tracking error was defined as $e(t) = \theta_{cmd}(t) - \theta(t)$.

Because the validated elevator-to-pitch plant has a negative steady-state gain, a positive nose-up pitch error requires a negative physical elevator command.

For proportional feedback, the corresponding physical control direction is therefore $\delta_e = -K_P e$.

This sign convention was retained throughout the P, PI, and PID designs.

4.3 Proportional Control

Proportional control was first investigated as the simplest feedback architecture.

A gain sweep was used to examine the effect of K_P on tracking error, overshoot, settling behavior, and elevator demand.

A representative proportional benchmark of $K_P = 2$ was selected.

For the 5° pitch command, the controller produced a final pitch angle of 3.2432°, corresponding to a steady-state tracking error of $\boxed{1.7568^\circ}$.

The maximum pitch response was 6.4128°, with approximately 28.26% command overshoot.

The 2% settling time relative to the controller's own final value was approximately 189.12 s.

Maximum absolute elevator demand reached 10.0°.

Proportional feedback therefore improved the aircraft response but could not provide accurate steady-state pitch tracking.

This result motivated the addition of integral action.

4.4 Proportional-Integral Control

Integral feedback was introduced to eliminate the persistent tracking error.

The control law was

$$\delta_e - \left(K_P e + K_I \int e\,, dt\right).$$

A two-parameter gain study was performed, and the selected PI benchmark used $K_P = 0.5$, $K_I = 0.3\ s^{-1}$.

The PI controller achieved $\theta_{ss} = 5.0000°$ with effectively zero steady-state error. The maximum pitch response was $6.3085°$, corresponding to 26.17% overshoot.

The 2% settling time decreased to approximately $67.01\ s$.

The long-duration maximum absolute elevator command was $5.4161°$.

An independent steady-state check was performed using the aircraft DC gain. Since $K_{DC} = -0.9230$, the elevator required to maintain a 5° pitch perturbation is approximately

$$\delta_{e,ss} \frac{5°}{-0.9230} \approx -5.417°.$$

The simulated long-duration PI elevator command converged to approximately $-5.416°$, providing an independent equilibrium check.

Integral action therefore solved the steady-state tracking problem, but overshoot and settling time remained relatively high.

4.5 Filtered PID Architecture

Derivative action was introduced to improve transient damping.

Rather than differentiating the pitch-command step directly, the derivative term was applied to the measured pitch angle using a first-order filtered derivative,

$$D(s) K_D \frac{s}{T_f s + 1}.$$

Applying derivative action to the measurement rather than directly to the reference reduces derivative kick at the instant of the step command.

The controller architecture therefore combined:

- proportional action on pitch error,
- integral action on pitch error,
- filtered derivative feedback from measured pitch angle.

A derivative-gain sweep was followed by a targeted multi-parameter study of (K_P), (K_I), and (K_D).

The initial ideal-actuator PID selected from this study used $K_P = 0.8$, $K_I = 0.5\ \mathrm{s}^{-1}$, $K_D = 0.8\ \mathrm{s}$, $T_f = 0.1\ \mathrm{s}$ and was carried forward for initial controller assessment.

4.6 Ideal-Actuator PID Performance

For the 5° pitch command, the selected PID achieved $\theta_{ss} = 5.0000°$ with effectively zero steady-state tracking error.

The maximum pitch angle was $5.9750°$, corresponding to $\boxed{19.50\%}$.

The peak occurred at approximately $4.0\ s$, and the 2% settling time was $\boxed{25.57\ \mathrm{s}}$.

Maximum long-duration elevator magnitude was approximately $5.4162°$.

The closed-loop poles were -8.9334, $-0.6556 \pm 1.0800i$, $-0.2472 \pm 0.2479i$, and -0.0111.

All poles have negative real parts, confirming closed-loop stability for the ideal-actuator design.

4.7 P, PI, and PID Comparison

The controller-development results are summarized below.

Table 2. P, PI, and PID Controller Performance Comparison

Metric	P	PI	PID
Final pitch (deg)	3.2432	5.0000	5.0000
Steady-state error (deg)	1.7568	≈0	≈0
Maximum pitch (deg)	6.4128	6.3085	5.9750
Overshoot (%)	28.256	26.171	19.499
2% settling time (s)	189.12	67.009	25.57
Maximum elevator magnitude (deg)	10.0000	5.4161	5.4162

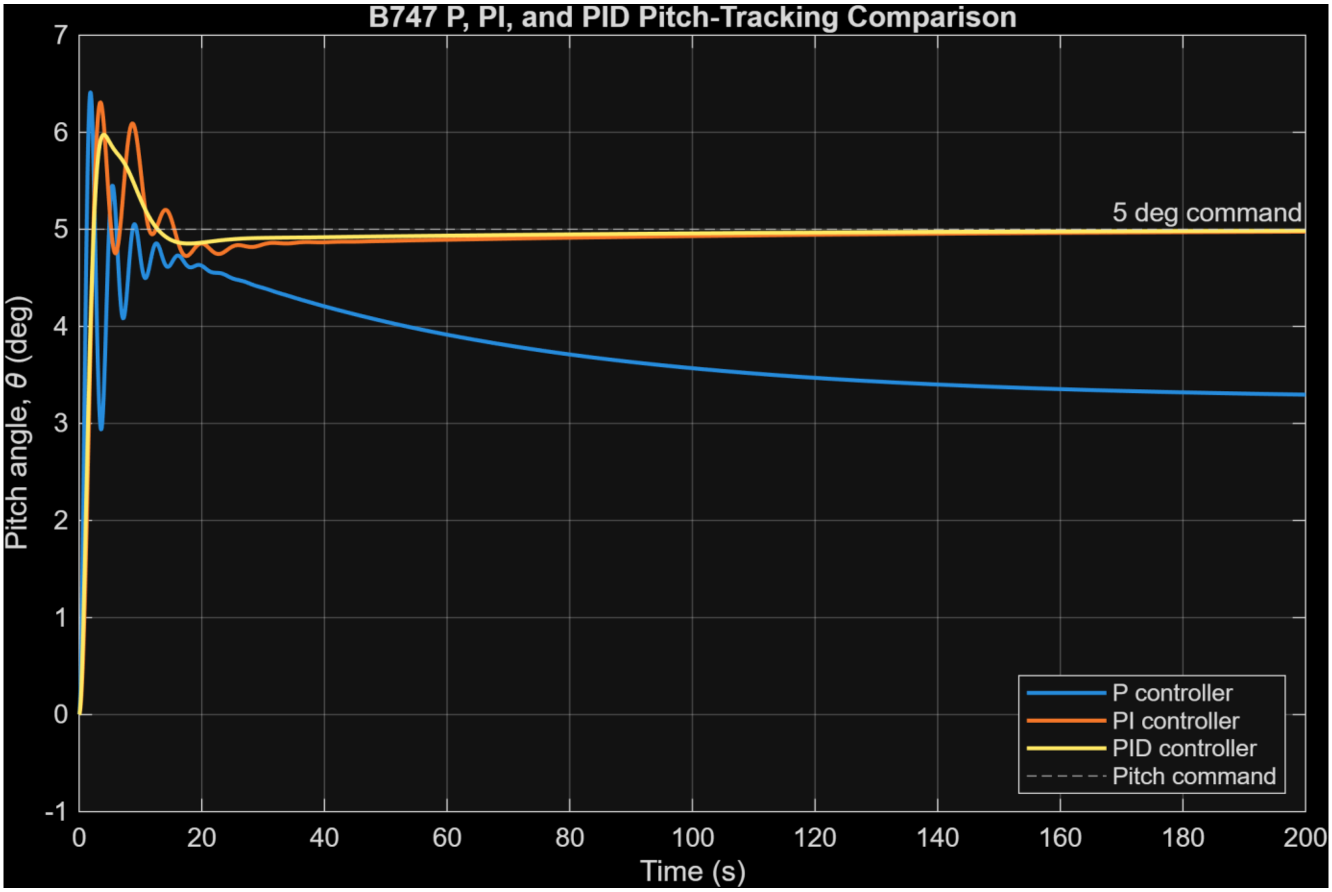

Figure 2. Comparison of proportional, proportional-integral, and filtered PID pitch responses to the 5° command. Integral action eliminates steady-state error, while derivative feedback substantially reduces overshoot and settling time.

The progression demonstrates the distinct contribution of each control term.

Proportional feedback provides immediate correction but retains substantial steady-state error.

Integral feedback eliminates this error by generating the persistent elevator bias required to maintain the commanded pitch.

Derivative feedback improves damping and allows substantially faster transient behavior while preserving zero steady-state error.

4.8 Quantitative Improvement of PID

Compared with the selected PI controller, PID reduced overshoot from 26.171% to 19.499% a reduction of approximately $\boxed{25.5\%}$. Settling time decreased from $67.009\ s$ to $25.57\ s$, corresponding to a reduction of approximately $\boxed{61.8\%}$.

Relative to the proportional benchmark, PID reduced settling time from $189.12\ s$ to $25.57\ s$, an improvement of approximately 86.5%.

Maximum elevator demand also decreased from $10.0°$ to approximately $5.42°$.

Most importantly, PID eliminated the $1.7568°$ steady-state error present under proportional control.

The source performance assessment therefore identified PID as the strongest overall classical architecture among the three designs evaluated.

4.9 Project Performance Screening

Two project-level transient targets were defined for the nominal $5°$ command: $M_p \leq 20\%$ and $t_s \leq 30$ s.

The selected ideal-actuator PID achieved $M_p = 19.499\%$ and $t_s = 25.57$ s.

It therefore satisfied both initial transient-performance screening targets while maintaining effectively zero steady-state error.

These thresholds are design criteria defined for comparison within this project and are not aircraft certification requirements.

4.10 Classical Controller Selection

The P controller was rejected because it retained substantial steady-state error and required the greatest elevator magnitude.

The PI controller eliminated steady-state error but retained relatively high overshoot and slow settling.

The filtered PID controller provided the best overall combination of

$$\boxed{\text{tracking accuracy} + \text{transient response} + \text{control effort}}$$

among the classical controllers investigated.

It was therefore selected as the classical baseline for subsequent disturbance, actuator, and robustness studies.

However, the PID selected in this section was designed assuming an ideal elevator actuator.

The next stages introduce realistic actuator dynamics, elevator travel limits, and elevator rate limits. As will be shown later, these physical constraints require the controller selection to be reassessed before the final actuator-aware PID is frozen.

5. MATLAB/Simulink Model Validation

5.1 Validation Objective

MATLAB and Simulink were both used extensively during controller development.

MATLAB provided a convenient environment for:

- state-space analysis,
- pole and eigenvalue calculations,
- controller design,
- gain studies,
- time-domain simulation,
- quantitative performance calculations.

Simulink was used to construct explicit signal-flow implementations of the aircraft and controllers and later to introduce actuator dynamics, rate limiting, travel saturation, and disturbances.

Because the two environments were used for different stages of the project, quantitative cross-validation was performed before relying on the Simulink models for subsequent engineering conclusions.

The objective was to verify that differences observed after introducing controllers or actuator nonlinearities resulted from the intended model changes rather than from inconsistent MATLAB and Simulink implementations.

5.2 Baseline Aircraft Simulink Model

The validated Boeing 747 longitudinal plant was transferred into Simulink using a State-Space block.

Rather than manually entering a second set of numerical coefficients, the Simulink model referenced the same MATLAB workspace variables used by the validated aircraft model: $A, \quad B_e, \quad C_\theta, \quad D_\theta.$

The baseline signal path consisted of:

$$elevator\ input \rightarrow unit\ conversion \rightarrow B747\ state - space\ plant \rightarrow pitch\ output.$$

The same $-1°$ elevator step used for the open-loop MATLAB analysis was applied in Simulink.

This ensured that both environments were evaluated using an identical aircraft model, input, initial condition, and simulation interval.

5.3 Numerical Comparison Method

The Simulink model used a variable-step numerical solver. Consequently, its output time samples were not identical to the uniformly specified MATLAB reference time vector.

A direct point-by-point subtraction of the raw outputs would therefore not provide a valid comparison.

Instead, the validation procedure:

1. loaded the frozen Boeing 747 aircraft model;
2. executed the Simulink simulation;

3. generated the corresponding MATLAB reference response;
4. aligned both solutions on a common time vector;
5. interpolated the variable-step Simulink result where necessary;
6. calculated point-by-point pitch-angle error;
7. evaluated maximum and root-mean-square disagreement.

The principal error quantities were $e_{\theta}(t)\theta_{\text{Simulink}}(t)\theta_{\text{MATLAB}}(t)$, the maximum absolute error, $e_{\max} \max|e_{\theta}(t)|$, and the root-mean-square error, $e_{\text{RMS}}\sqrt{\frac{1}{N}\sum_{i=1}^{N} e_{\theta}^{2}\,(t_i)}$.

5.4 Baseline Aircraft Validation Results

For the 400-second open-loop aircraft simulation, the MATLAB and Simulink results showed extremely close agreement.

The measured discrepancies were approximately $\boxed{e_{\max} 6.31 \times 10^{-4}\,{}^{\circ}}$ and $\boxed{e_{\text{RMS}} 3.19 \times 10^{-5}\,{}^{\circ}}$.

Relative to the peak aircraft pitch response, these corresponded to approximately 0.0103% maximum relative error and 0.00052% RMS relative error.

The two response curves were effectively coincident at the scale of the aircraft motion.

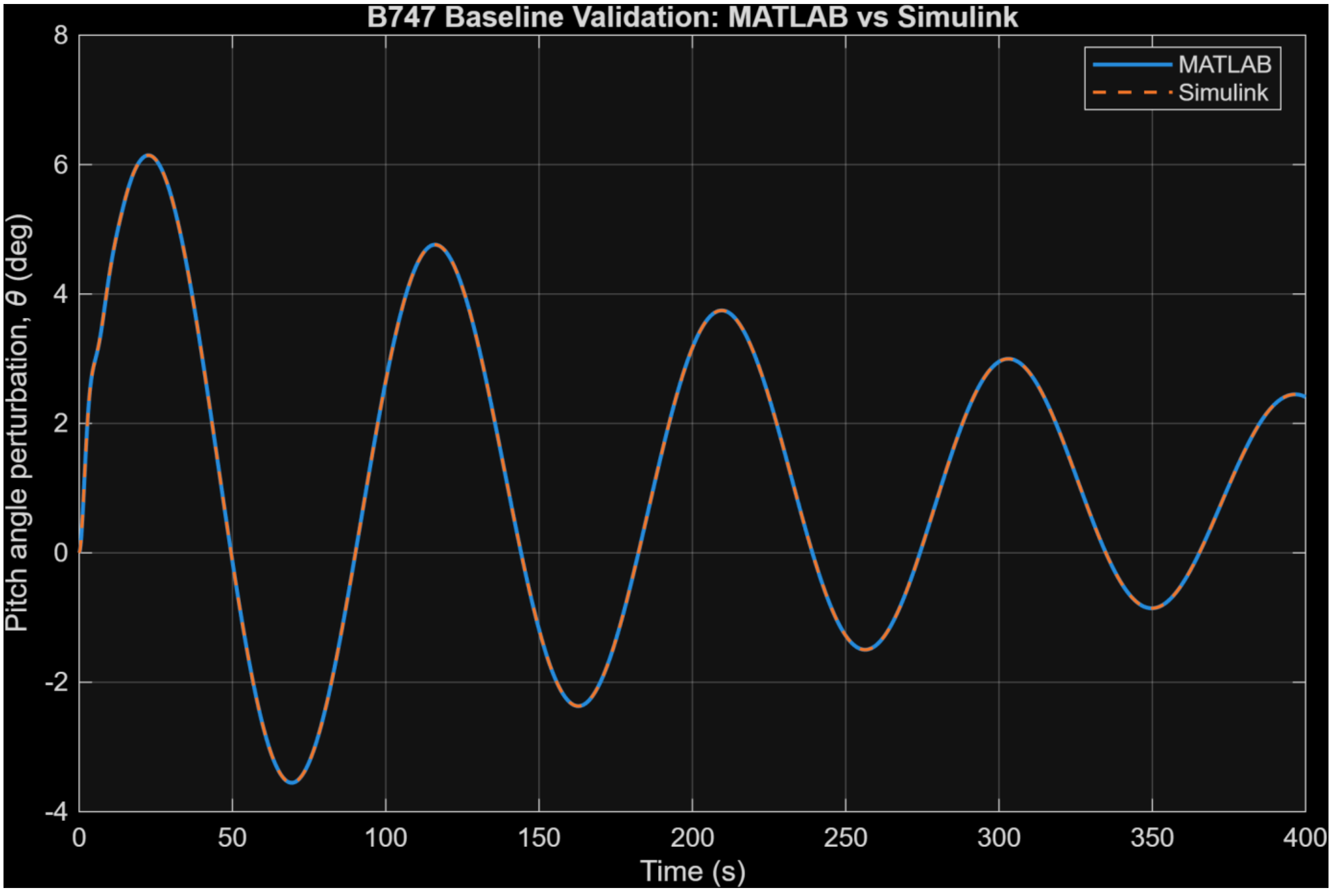

Figure 3. MATLAB and Simulink open-loop Boeing 747 pitch responses for the same elevator input. The nearly coincident responses demonstrate numerical consistency between the two implementations.

The small remaining discrepancy is negligible relative to the aircraft response and is consistent with numerical integration and interpolation differences.

The Simulink aircraft model was therefore accepted as a validated implementation of the MATLAB baseline plant.

5.5 PID Implementation Validation

The filtered PID architecture developed in Section 4 was also implemented explicitly in Simulink.

Rather than using a single preconfigured PID block, the model contained separate:

- proportional error feedback,
- integral error feedback,
- filtered derivative feedback from measured pitch,
- controller-output summation,

- aircraft state-space dynamics.

This made the implemented control law directly traceable to the MATLAB controller formulation.

The MATLAB and Simulink PID pitch responses were again aligned on a common time vector and compared point by point.

The maximum absolute pitch discrepancy was approximately 1.85×10^{-3} ° and the RMS discrepancy was approximately 1.36×10^{-4} °.

Relative to the peak pitch response, the maximum disagreement was approximately 0.0310% with RMSrelative disagreement of approximately 0.00228% . These errors are negligible relative to the aircraft pitch response.

The MATLAB analytical controller model and explicit Simulink block-diagram implementation were therefore considered numerically consistent.

5.6 LQI Architecture Validation

A similar MATLAB–Simulink comparison was performed when the LQI architecture was introduced later in the project.

For the validated LQI implementation, the maximum pitch-angle discrepancy was approximately 6.15×10^{-8} ° with RMS pitch error of approximately 8.19×10^{-9} °.

The maximum discrepancy in the requested elevator command was approximately 5.09×10^{-8} °, while the maximum discrepancy in actual first-order-actuator elevator response was approximately 6.72×10^{-6} °.

These differences are essentially numerical.

This validation confirmed the correctness of the LQI Simulink signal architecture before the subsequent structured LQI weight-tuning study.

The final tuned LQI configuration was later evaluated using the complete actuator-constrained Simulink model and independently checked again during the final system-validation phase.

5.7 Reproducibility

Dedicated MATLAB scripts were created to automate the MATLAB–Simulink validation procedures.

The scripts load the frozen aircraft model, execute the required Simulink model, generate the MATLAB reference solution, align the time histories, calculate numerical discrepancies, and export the resulting comparison plots.

This reduces dependence on manually retained workspace variables and allows the validation calculations to be repeated from a fresh MATLAB session.

The baseline aircraft is stored separately as B747_longitudinal_baseline.mat, while the final controller configuration is frozen later in the project as final_control_configuration.mat.

This separation provides a consistent chain from the validated aircraft model to the final controller simulations.

5.8 Validation Outcome

The independent MATLAB and Simulink implementations produced negligible discrepancies for the baseline aircraft, classical PID controller, and LQI control architecture.

The validation therefore supports the following conclusion: MATLAB and Simulink implementations are numerically consistent for the models tested.

This cross-validation is important because the remainder of the project introduces effects that are most naturally implemented in Simulink, including actuator dynamics, nonlinear travel and rate limits, external disturbances, and uncertain aircraft control effectiveness.

Consequently, later changes in system response can be interpreted as effects of the intended controller or physical-model modifications rather than as baseline software-implementation mismatch.

6. Actuator Dynamics and Physical Constraints

6.1 Motivation

The classical controller development in Section 4 initially assumed that commanded elevator motion could be applied directly to the aircraft.

A real elevator actuator cannot respond instantaneously and is subject to limits on both control-surface travel and deflection rate.

To increase the physical realism of the simulation, a documented Boeing 747-100/200 elevator-actuator representation was introduced and the previously selected PID controller was reevaluated.

Three actuator effects were considered:

• first-order actuator dynamics,

• finite elevator travel,

• finite elevator rate.

This step was necessary because satisfactory aircraft pitch response does not automatically imply that the required control-surface motion is physically achievable.

6.2 Elevator Actuator Model

The elevator actuator was modeled as the first-order transfer function $A(s) = \frac{\delta_e(s)}{\delta_{e,cmd}(s)} = \frac{37}{s+37}$.

The corresponding time constant is $\tau_a = \frac{1}{37} = 0.0270\ s$. The adopted elevator travel limits were $-23° \leq \delta e \leq +17°$, with a maximum deflection-rate magnitude of $|\dot{\delta}_e| \leq \frac{37°}{s}$

These parameters were adopted from a documented B747-100/200 actuator representation.

The actuator source is separate from the MIT Boeing 747 longitudinal state-space source used for the baseline aircraft dynamics. The actuator values are therefore treated as documented B747 actuator constraints adopted for this study rather than as a claim that both source models represent the identical aircraft configuration.

6.3 Effect of First-Order Actuator Lag

The actuator transfer function was first introduced without travel or rate saturation.

The ideal-elevator and first-order-actuator responses were:

Table 3. Ideal-Elevator and First-Order-Actuator Performance Comparison

Metric	Ideal Elevator	First-Order Actuator
Final Pitch	5.0000°	5.0000°
Maximum Pitch	5.9750°	5.9895°
Overshoot	19.50%	19.79%
Peak time	4.02 s	3.98 s
2% settling time	25.57 s	25.48 s

The maximum point-by-point pitch-response difference was only 0.0465°.

Thus, actuator lag alone produced only a minor change in pitch response.

This is consistent with the short actuator time constant, $\tau a \approx 0.027s$, which is much faster than the dominant aircraft longitudinal dynamics.

6.4 Initial Actuator Feasibility Audit

Although the pitch response changed very little, the physical elevator motion revealed a substantially different result.

For the nominal $0° \rightarrow 5°$ pitch command, the unconstrained first-order actuator reached approximately $\delta e_{min} = -4.1368°$ and $\delta e_{max} \approx 0°$.

These values were comfortably within the adopted travel limits. Therefore, Elevator travel: PASS

However, the predicted maximum actuator rate was approximately 148°/s.

Compared with the adopted physical rate limit, 37°/s, the unconstrained model demanded approximately $\frac{148}{37} = 4$ times the available rate capability. Therefore, Elevator rate: FAIL

This was a significant result: examining pitch angle alone would have suggested that the actuator model had little effect, while direct inspection of surface motion exposed a genuine feasibility problem.

6.5 Nonlinear Actuator Model

The Simulink model was therefore expanded to include the complete actuator chain:

$$\mathrm{PID} \rightarrow \frac{37}{s+37} \rightarrow \text{Rate Limiter} \rightarrow \text{Travel Saturation} \rightarrow \text{Aircraft}$$

The actuator constraints were $-\frac{37^\circ}{\mathrm{s}} \le \dot{\delta}_e \le \frac{37^\circ}{\mathrm{s}}$ and $-\frac{37^\circ}{\mathrm{s}} \le \dot{\delta}_e \le \frac{37^\circ}{\mathrm{s}}$.

Both the controller-requested elevator and the actual actuator output were recorded so that command demand and physically delivered control motion could be evaluated separately.

6.6 Original PID Under Physical Constraints

The ideal-actuator PID from Section 4 was $Kp = 0.8,\ Ki = 0.5,\ Kd = 0.8,\ Tf = 0.1s$. This controller was first tested without retuning.

Once the nonlinear actuator constraints were enforced, the system produced approximately $\theta_{max} = 6.0171°$, corresponding to 20.342% overshoot, with a settling time of 25.474 s.

The elevator remained within its travel range, and the rate limiter correctly constrained actuator motion to 37°/s. However, 20.342% > 20%, so the controller slightly violated the previously established overshoot screening criterion.

This meant that the controller selected under an ideal-actuator assumption could not simply be accepted as the final design once physical actuator behavior was included.

6.7 Actuator-Aware PID Reassessment

Three previously identified PID candidates were retested using the complete constrained actuator model.

Table 4. Actuator-Aware PID Candidate Comparison

Candidate	K_P	K_I	K_D	Overshoot	Settling time	Travel	Rate
A	0.8	0.5	0.8	20.342%	25.474 s	PASS	PASS
B	1.0	0.5	0.8	15.881%	27.074 s	PASS	PASS
C	1.0	0.6	1.0	20.259%	21.166 s	PASS	PASS

Candidate B was the only tested controller that simultaneously satisfied $Mp \leq 20$, $t_s \leq 30s$, the elevator travel limits, and the elevator rate constraint. The final actuator-aware PID was therefore selected as $k_P = 1.0$, $k_I = 0.5$, $K_d = 0.8$, $T_f = 0.1s$.

This controller replaces the earlier ideal-actuator PID as the final classical benchmark used for the remainder of the project.

6.8 Final Actuator-Aware PID Performance

For the nominal 5° pitch command, the final constrained controller produced $\theta_{(max)} = 5.7941°$, with 15.881% overshoot. The peak occurred at approximately 3.3434 s, and the 2% settling time was 27.074 s.

The controller requested a minimum elevator command of approximately -5.2183°, while the physical actuator reached -5.1990°.

Maximum actuator rate was 37.000°/s, equal to the imposed rate limit. Therefore,

Travel-limit check: PASS

Rate-limit check: PASS

Nominal performance screening: PASS

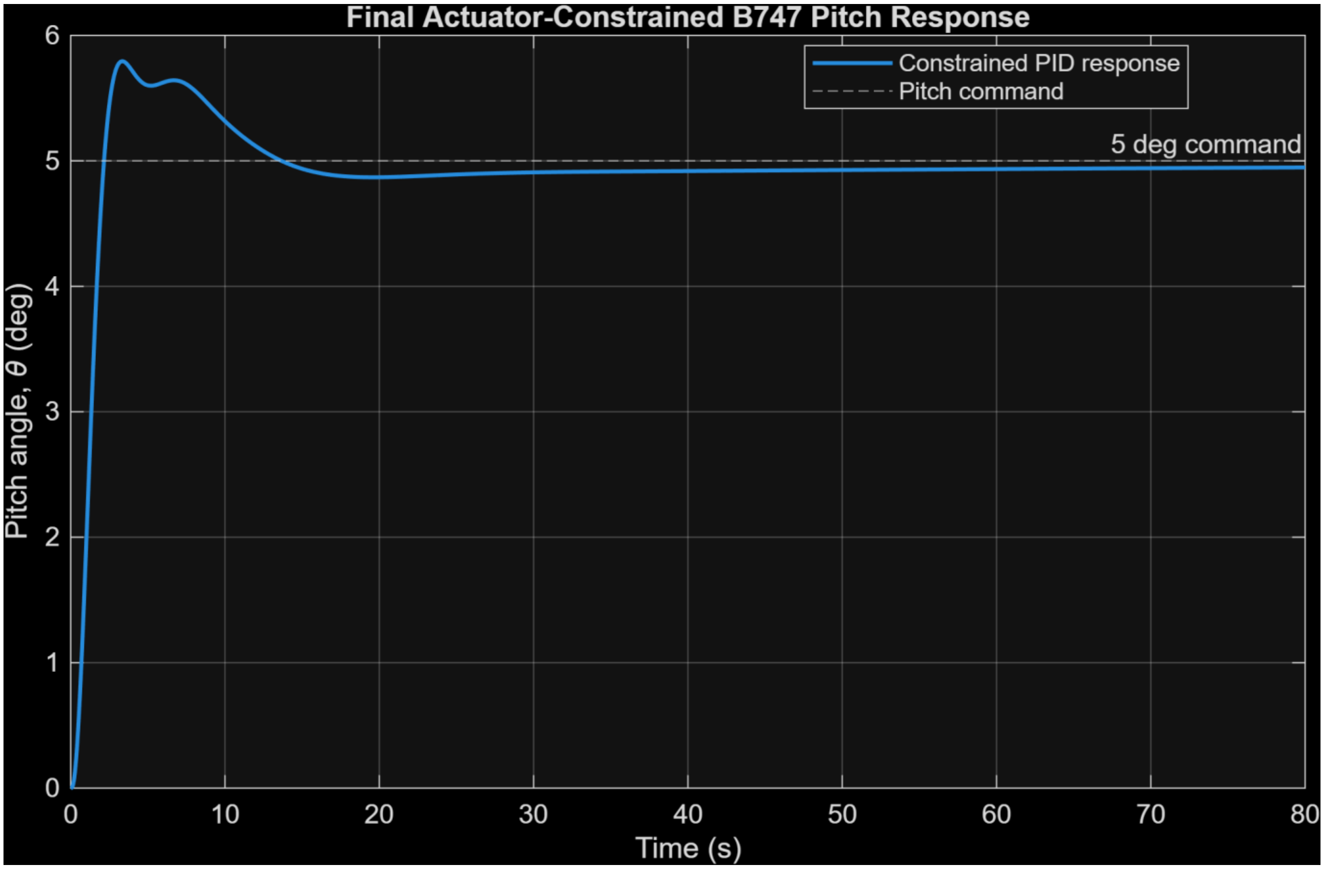

Figure 4. Final actuator-constrained Boeing 747 pitch response using the actuator-aware PID controller. The controller satisfies the nominal project overshoot and settling-time criteria while respecting the adopted actuator limits.

6.9 Requested Versus Actual Elevator Motion

The largest difference between requested and actual elevator position occurred immediately after the pitch-command step.

The controller initially requested rapid elevator motion, while the physical actuator was restricted by the 37°/s rate limit. The maximum command-to-actuator mismatch was approximately 5°.

The rate limiter was active for only approximately 0.139 s, and the travel-saturation block was active for 0 s.

Therefore, the nominal maneuver was rate-limited briefly but never travel-saturated.

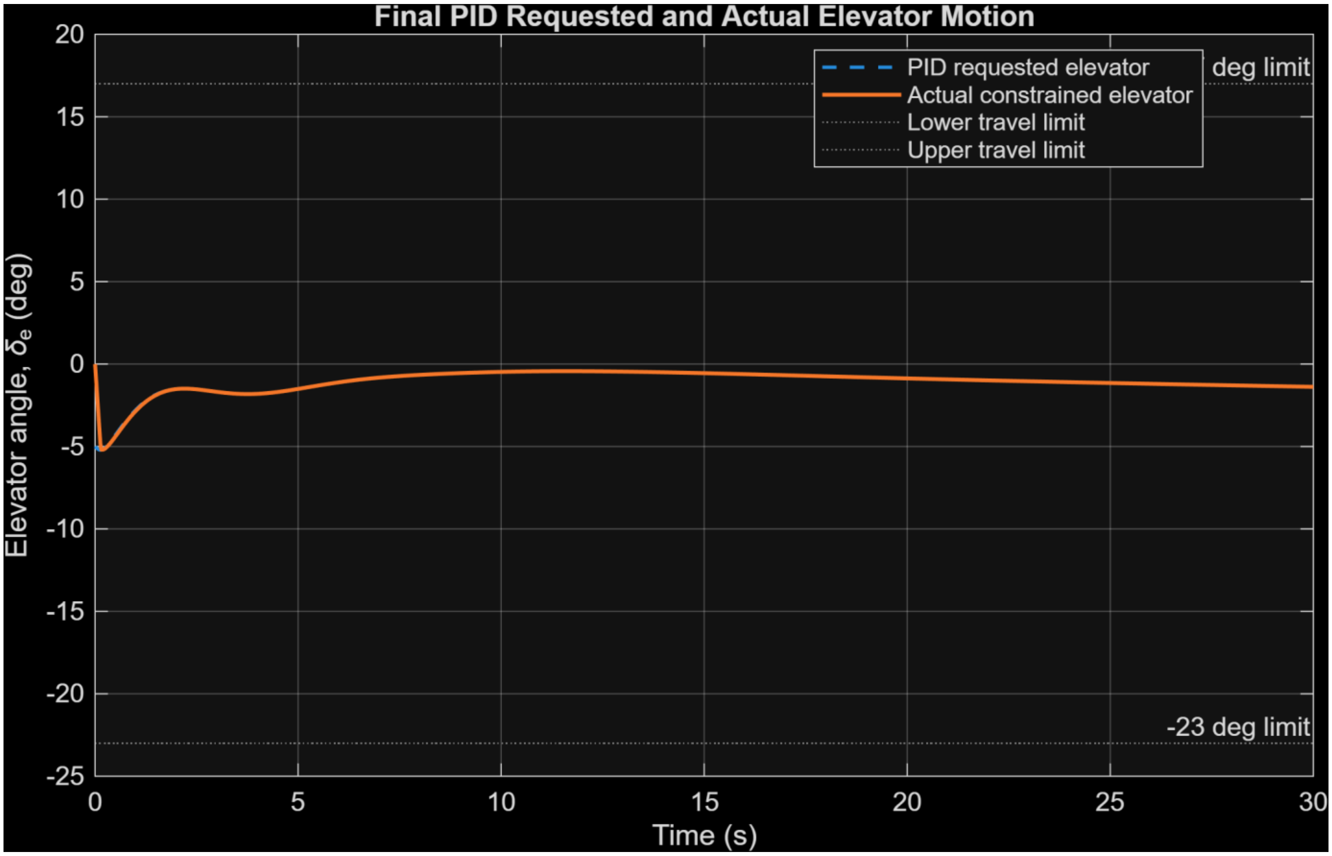

Figure 5. PID-requested elevator command and actual constrained elevator motion. The initial discrepancy results from the actuator-rate constraint, after which the requested and delivered elevator responses converge.

6.10 Anti-Windup Assessment

Because the PID contains integral action, actuator limiting creates the possibility of integrator windup. This possibility was evaluated explicitly.

For the nominal maneuver:

• travel saturation did not occur,

• rate saturation was brief,

• no sustained actuator-command mismatch developed,

• no significant windup behavior was observed.

The nonlinear constraints increased overshoot only modestly, while settling time remained essentially unchanged. An additional anti-windup subsystem was therefore not introduced for the baseline PID configuration. This was a modeling decision based on the simulated actuator behavior rather than an assumption that anti-windup is generally unnecessary.

6.11 Engineering Interpretation

The actuator study changed the interpretation of the controller design in two important ways.

First, the first-order actuator lag itself had almost no effect on aircraft pitch response. If evaluation had stopped there, the ideal-actuator controller might have appeared physically acceptable.

However, direct examination of elevator motion showed that the unconstrained actuator would require approximately 148°/s, four times the adopted physical rate capability.

Second, enforcing the nonlinear rate constraint slightly changed the aircraft response enough that the previously selected ideal-actuator PID no longer met the project's overshoot criterion. The controller therefore had to be reassessed with the physical actuator included in the design loop.

$$\text{Ideal Controller Design} \rightarrow \text{Actuator Feasibility Audit} \rightarrow \text{Constraint Violation} \rightarrow \text{Controller Reassessment} \rightarrow \text{Feasible Final PID}$$

The final actuator-aware PID was $k_P = 1.0$, $k_I = 0.5$, $K_d = 0.8$, $T_f = 0.1s$ and is therefore adopted as the final classical controller for subsequent disturbance and robustness analysis.

7. Disturbance Rejection

7.1 Objective

The disturbance-rejection analysis evaluated the ability of the pitch-control system to maintain the commanded aircraft attitude when subjected to a temporary control-channel disturbance.

The aircraft was commanded to maintain $\theta_{\text{cmd}} = 5°$ while a temporary positive elevator disturbance was applied from $t = 40$ s to $t = 42$ s, giving a disturbance duration of $\Delta t_d = 2$ s.

Under the adopted aircraft sign convention, positive elevator deflection represents elevator-down motion. Therefore, the imposed positive disturbance acts in a direction that temporarily drives the aircraft away from the commanded nose-up pitch condition.

An additive control-channel disturbance was selected because it provides a controlled and physically interpretable test of feedback rejection capability without requiring an additional aerodynamic gust model.

The disturbance test should therefore be interpreted as a **control-channel disturbance-rejection study**, rather than as a complete representation of atmospheric turbulence or aerodynamic gust loading.

7.2 Preliminary Unconstrained Disturbance Study

Disturbance rejection was first investigated before physical actuator constraints were introduced.

The initial PID used in this preliminary study was $K_p = 0.8$, $K_I = 0.5$, $K_d = 0.8$, $T_f = 0.1s$.

Two disturbance amplitudes were evaluated: $\delta_{e,d} = +1°$ and $\delta_{e,d} = +2°$, with both disturbances applied over $40 \leq t < 42$ s.

The total physical elevator input was represented as $\delta_{e,\text{total}}(t)\delta_{e,\text{controller}}(t) + \delta_{e,\text{disturbance}}(t)$.

Because the aircraft and controller models were linear at this stage, the total pitch response could also be interpreted using superposition: $\theta_{\text{total}}(t)\theta_{\text{nominal}}(t) + \theta_{\text{disturbance}}(t)$.

This allowed the incremental influence of the disturbance to be evaluated separately from the nominal pitch-command response.

7.3 Preliminary Disturbance Results

For the $\delta_{e,d} = +1°$ disturbance, the maximum deviation from the commanded pitch was $|\theta - \theta_{\text{cmd}}|_{\max} 0.7436°$, occurring at approximately $t = 42.05$ s.

The disturbance-only contribution reached $|\theta_d|_{\max} = 0.6640°$.

A recovery band corresponding to 2% of the 5° pitch command was defined as $5° \pm 0.1°$, or equivalently, $4.9° \leq \theta \leq 5.1°$.

Following disturbance removal, the aircraft returned permanently to this band after approximately $t_{\text{rec}} = 4.80$ s.

The maximum additional PID elevator action was $\Delta\delta_{e,\text{PID}} - 0.9853°$, which corresponds to approximately $\eta_{\text{comp}} \frac{0.9853}{1.0000} \times 10098.53$ % peak disturbance compensation.

When the disturbance magnitude was doubled to $\delta_{e,d} = +2°$, the maximum pitch-command deviation increased to $|\theta - \theta_{\text{cmd}}|_{\max} 1.4076°$.

The recovery time increased to $t_{\text{rec}} = 5.95$ s, and the maximum additional PID action increased to $\left|\Delta\delta_{e,\text{PID}}\right|_{\max} 1.9706°$.

The preliminary disturbance results are summarized below.

Table 5. Preliminary Disturbance-Rejection Results

Metric	+1° Disturbance	+2° Disturbance
Disturbance duration	2.00 s	2.00 s
Maximum pitch deviation	0.7436°	1.4076°
Time of maximum deviation	42.05 s	42.05 s
Recovery band	±0.100°	±0.100°
Recovery time	4.80 s	5.95 s
Maximum additional PID action	0.9853°	1.9706°
Peak disturbance compensation	98.53%	98.53%
Closed-loop response	Stable	Stable

Doubling the disturbance approximately doubled the required incremental controller action: $1.9706° \approx 2(0.9853°)$.

This behavior is consistent with the linear aircraft and controller model used during the preliminary disturbance study.

The result should therefore be interpreted as confirmation of approximately linear disturbance-response scaling rather than as evidence of robustness to nonlinear aircraft behavior or model uncertainty.

7.4 Actuator-Constrained Disturbance Model

The preliminary analysis did not yet establish physical actuator feasibility.

After the realistic actuator model was introduced, disturbance rejection was repeated using the final actuator-aware PID: $K_P = 1.0, K_I = 0.5, K_D = 0.8, T_f = 0.1$ s.

The actuator dynamics were $A(s) = \frac{37}{s+37}$, with travel limits $-23^\circ \le \delta_e \le 17^\circ$, and rate limit $|\dot{\delta}_e| \le \frac{37^\circ}{\text{s}}$.

The constrained controller signal path was $\text{PID} \rightarrow \frac{37}{s+37} \rightarrow \text{Rate Limiter} \rightarrow \text{Travel Saturation} \rightarrow \text{Aircraft}$.

The additive disturbance was introduced at the aircraft control input after the actuator.

Therefore, the actuator constraints apply to the **corrective elevator motion generated by the controller**, while the disturbance represents an external additive control-channel perturbation.

7.5 Constrained $+1^\circ$ Disturbance

For the constrained disturbance $\delta_{e,d} = +1^\circ$, the maximum pitch deviation from the 5° command was approximately $|\theta - \theta_{\text{cmd}}|_{\max} 0.7051^\circ$.

The largest deviation occurred at approximately $t = 42.03$ s.

The disturbance-only contribution reached approximately $|\theta_d|_{\max} 0.6254^\circ$.

Following disturbance removal, the aircraft returned permanently to the $5^\circ \pm 0.1^\circ$ recovery region after approximately $t_{\text{rec}} 4.14$ s.

The physical actuator remained within both its travel and rate limits.

Therefore, $\text{Travel Limit: PASS}$ and Rate Limit: PASS.

7.6 Constrained $+2^\circ$ Disturbance

The stronger final disturbance case used $\delta_{e,d} = +2^\circ$. From $40 \le t < 42$ s.

The maximum deviation of the complete aircraft response from the 5° command was $|\theta - \theta_{\text{cmd}}|_{\max} 1.3305^\circ$.

The isolated disturbance contribution reached $|\theta_d|_{\max} 1.2507^\circ$.

The aircraft returned permanently to the $5^\circ \pm 0.1^\circ$ recovery region after approximately $t_{\text{rec}} 5.4855$ s.

The closed-loop aircraft remained stable throughout the disturbance and subsequent recovery.

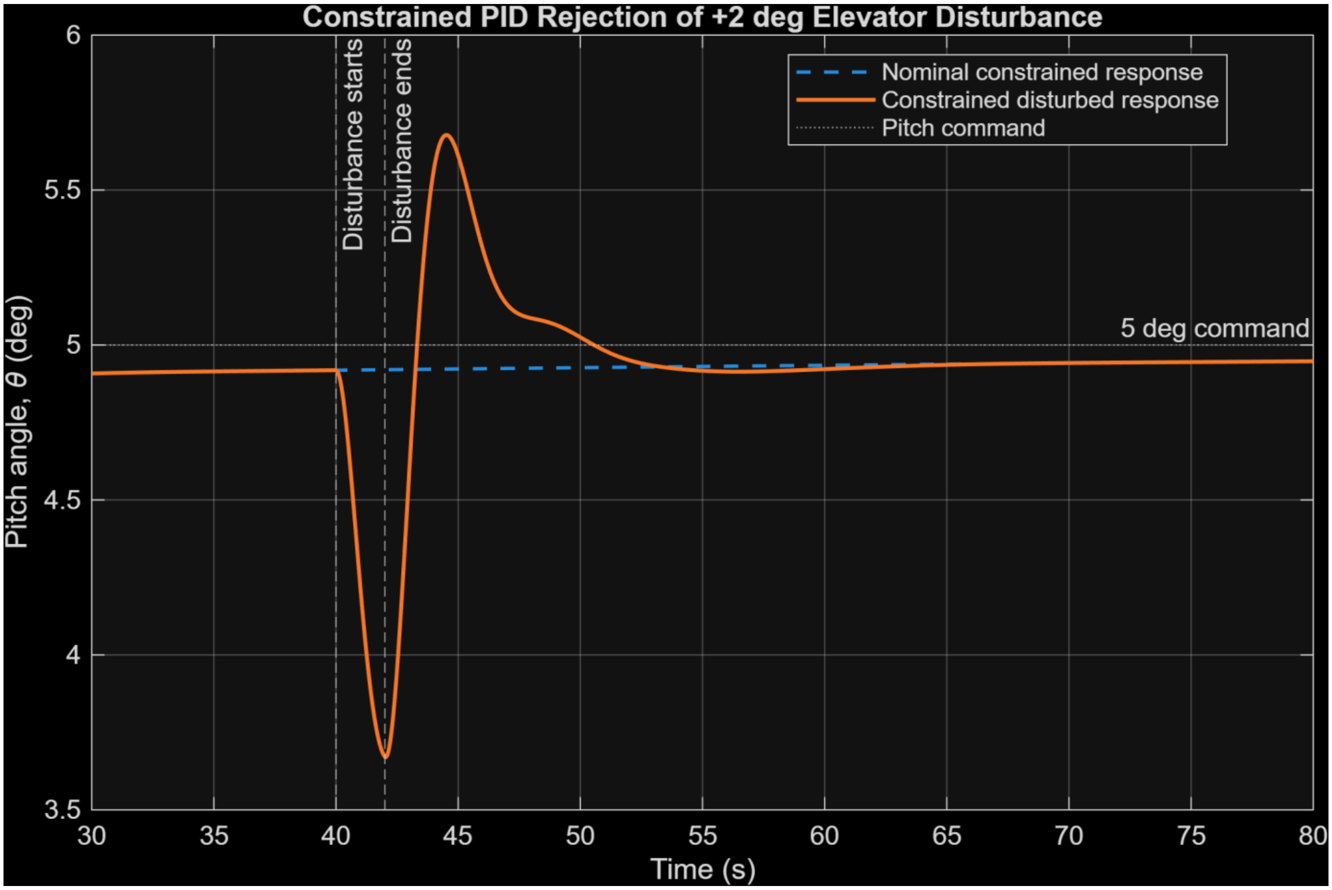

Figure 6. Actuator-constrained pitch response to a (+2^\circ), 2-second additive control-channel disturbance. The closed-loop aircraft remains stable and returns to the commanded pitch following disturbance removal.

7.7 Actuator Demand During Disturbance Rejection

The overall maximum actuator rate during the complete $+2^\circ$ simulation was $\frac{|\dot{\delta}e|\text{max}37^\circ}{\text{s}}$.

However, this maximum occurred during the initial 5° pitch-command maneuver rather than during the disturbance itself.

During the disturbance and subsequent recovery period, the maximum actuator rate was only approximately $\frac{|\dot{\delta}e|\ \text{max,dist}2.0757^\circ}{\text{s}}$.

Relative to the available actuator-rate capability,

$$\frac{2.0757}{37} \times 100 \approx 5.61\%$$

Thus, rejection of the tested $+2^\circ$ disturbance required only approximately **5.61% of the available elevator-rate capability** once the aircraft was near its commanded operating condition.

Both actuator checks remained satisfied: $\text{Travel Limit: PASS}$, $\boxed{\text{Rate Limit: PASS}}$.

7.8 Preliminary and Constrained Comparison

The preliminary and actuator-constrained (+2^\circ) disturbance cases are summarized below.

Table 6. Preliminary and Actuator-Constrained Disturbance Comparison

Metric	Preliminary PID	Final Constrained PID
Kp	0.8	1.0
Ki	0.5	0.5
Kd	0.8	0.8
Disturbance amplitude	+2°	+2°
Disturbance duration	2.00 s	2.00 s
Maximum total pitch deviation	1.4076°	1.3305°
Disturbance-only pitch peak	—	1.2507°
Recovery time	5.95 s	5.4855 s
Actuator constraints included	No	Yes
Closed-loop response	Stable	Stable

The constrained result is treated as the primary engineering result because it uses the final actuator-aware PID and includes the physical actuator model.

The earlier unconstrained analysis remains useful for demonstrating the controller's opposing action and approximately linear response to increasing disturbance magnitude.

7.9 Engineering Interpretation

The disturbance analysis was intentionally developed in two stages.

The preliminary linear study demonstrated that the PID controller generated the correct opposing control action and that increasing disturbance amplitude produced approximately proportional increases in pitch deviation and corrective elevator demand.

However, that analysis did not establish whether the required controller action was physically achievable.

The actuator-constrained simulations therefore provide the more important engineering result.

For the selected $\delta_{e,d} = +2^\circ$ disturbance, the final actuator-aware PID limited the disturbance-only pitch effect to $|\theta_d|_{\max} 1.2507^\circ$ and restored the aircraft to within $\pm 0.1^\circ$ of the commanded pitch in approximately 5.4855 s.

The controller remained stable and respected the adopted actuator travel and rate constraints.

Furthermore, the maximum actuator rate required specifically during disturbance rejection was only $\frac{2.0757^\circ}{\text{s}}$, compared with the available $\frac{37^\circ}{\text{s}}$ rate capability.

The final disturbance study therefore demonstrates that the actuator-aware PID can reject the tested short-duration control-channel disturbances without exhausting the modeled actuator capability.

This conclusion remains limited to the disturbance model used in the project. The analysis does not explicitly represent atmospheric turbulence, aerodynamic gusts, sensor disturbances, structural disturbances, or the complete disturbance environment of an actual aircraft.

The disturbance test should therefore be interpreted as a controlled evaluation of **closed-loop rejection capability within the longitudinal simulation framework**, rather than as a complete flight-disturbance qualification.

8. Robustness and Sensitivity Analysis

8.1 Objective

The robustness study evaluated how sensitive the final actuator-aware PID controller was to uncertainty in the aircraft model.

The controller gains were held fixed at $K_P = 1.0, K_I = 0.5, K_D = 0.8, T_f = 0.1$ s.

The actuator model and physical limits were also retained: $A(s) = \frac{37}{s+37}, -23^\circ \leq \delta_e \leq 17^\circ$, and $|\dot{\delta}_e| \leq \frac{37^\circ}{\mathrm{s}}$.

Two aircraft-model characteristics were investigated:

- elevator control effectiveness,
- pitch-rate damping.

Each was varied by up to $\pm 20\%$ about its nominal value.

These variations were selected as **engineering sensitivity cases** for the present project. They should not be interpreted as certified Boeing 747 uncertainty bounds.

The controller was not retuned for any individual uncertainty case. This allowed the analysis to evaluate the sensitivity of the fixed final design.

8.2 Robustness Evaluation Criteria

The same project-level transient screening requirements used during controller development were retained: $M_p \leq 20\%$ and $t_s \leq 30$ s.

The nonlinear simulations were also checked against the physical actuator requirements: $-23^\circ \leq \delta_e \leq 17^\circ$ and $|\dot{\delta}_e| \leq \frac{37^\circ}{\mathrm{s}}$.

The robustness analysis therefore distinguished between three different concepts:

- **closed-loop stability** — whether the response remained bounded and convergent;
- **actuator feasibility** — whether elevator travel and rate limits remained satisfied;
- **transient-performance compliance —** whether overshoot and settling-time targets were met.

A case could therefore remain stable and physically feasible while still failing one of the selected transient-performance criteria.

8.3 Elevator-Effectiveness Sensitivity

The elevator input vector determines how strongly elevator deflection influences the aircraft longitudinal states.

Elevator effectiveness was varied by scaling the nominal input vector: $B_{e,\mathrm{test}}\lambda_e B_{e,\mathrm{nom}}$, where $\lambda_e \in 0.8,\ 0.9,\ 1.0,\ 1.1,\ 1.2.$

These values represent $-20\%,\ -10\%,\ 0\%,\ +10\%,\ +20\%$ changes in elevator effectiveness.

The first sensitivity sweep retained the first-order actuator dynamics but did not yet apply the nonlinear travel and rate limits.

The results were:

Table 7. Elevator-Effectiveness Sensitivity Results

Elevator Effectiveness	Final Pitch	Overshoot	Peak Time	2% Settling Time	Stable
-20%	5.000°	14.150%	7.32 s	40.734	PASS
-10%	5.000°	14.313%	3.48 s	30.984 s	PASS
Nominal	5.000°	14.912%	3.34 s	27.077 s	PASS
+10%	5.000°	15.305%	3.22 s	24.182 s	PASS
+20%	5.000°	15.544%	3.14	21.286 s	PASS

All tested cases remained stable and retained effectively zero steady-state tracking error.

Overshoot also remained below the project limit of 20% for every tested elevator-effectiveness case.

However, reduced elevator effectiveness substantially increased settling time.

For a 20% reduction, $t_s = 40.734$ s while a 10% reduction produced $t_s = 30.984$ s.

Both exceed the selected 30 s settling-time target.

The controller was therefore significantly more sensitive to **loss of elevator effectiveness** than to an equivalent increase in control effectiveness.

8.4 Weak-Elevator Cases with Full Actuator Constraints

The reduced-effectiveness cases were then repeated using the complete nonlinear actuator model.

The results were:

Table 8. Weak-Elevator Cases with Full Actuator Constraints

Case	Overshoot	Peak Time	Settling Time	Minimum Elevator	Maximum Rate	Travel

-20% effectiveness	14.328%	3.6688 s	40.730 s	-5.2365°	37°/s	PASS
-10% effectiveness	15.245%	3.4836 s	30.962 s	-5.2162°	37°/s	PASS
Nominal	15.881%	3.3434 s	27.074 s	-5.1990°	37°/s	PASS

The nonlinear results were almost identical to the earlier sensitivity prediction.

In the worst weak-elevator case, $\delta_{e,\min} = -5.2365°$, which remains far from the available lower travel boundary of $-23°$.

The actuator-rate constraint also remained satisfied.

Therefore, the poor settling performance was **not caused by elevator saturation or insufficient actuator capability**.

Instead, reduced aircraft control effectiveness was the dominant cause.

This distinction is important: weak-elevator cases were performance-limited, not actuator-limited

8.5 Pitch-Rate-Damping Sensitivity

The second uncertainty study investigated changes in the aircraft's natural pitch-rate damping.

The nominal pitch-rate damping term appears in the pitch-rate equation through the state-space coefficient associated with (q).

Its magnitude was varied using $A_{33,\mathrm{test}}\lambda_q A_{33,\mathrm{nom}}$, where $\lambda_q \in 0.8,\ 0.9,\ 1.0,\ 1.1,\ 1.2$.

A value below unity represents reduced damping magnitude, while a value above unity represents increased damping magnitude.

The resulting responses were:

Table 9. Pitch-Rate-Damping Sensitivity Results

Pitch-Damping Change	Final Pitch	Overshoot	Peak Time	2% Settling Time	Stable
-20%	5.000°	15.765%	3.16 S	27.090 S	PASS
-10%	5.000°	15.287%	3.24 S	27.085 S	PASS
Nominal	5.000°	14.912%	3.34 S	27.077 S	PASS
+10%	5.000°	14.648%	3.46 S	27.068	PASS
+20%	5.000°	14.503%	3.60 S	27.056	PASS

All tested pitch-damping cases remained stable.

All also satisfied both project performance requirements.

Reduced damping produced a modest increase in overshoot, while increased damping slightly reduced overshoot.

However, settling time changed only minimally across the entire $\pm 20\%$ range.

The final PID therefore demonstrated comparatively low sensitivity to the tested pitch-rate-damping variation.

8.6 Combined Uncertainty Corner Study

Elevator-effectiveness and pitch-damping variations were then applied simultaneously.

Rather than evaluating every possible combination, the extreme uncertainty corners were tested:

- weak elevator + low damping,
- weak elevator + high damping,
- strong elevator + low damping,
- strong elevator + high damping.

The nominal system was retained as a reference.

The complete nonlinear actuator model remained active throughout this study.

Table 10. Combined-Uncertainty Results

Case	Overshoot	Peak Time	Settling Time	Minimum Elevator	Maximum Rate	Travel
Nominal	15.881%	3.3434 s	27.074 s	-5.1990°	37°/s	PASS
Weak elevator + low damping	15.285%	3.4421 s	40.774 s	-5.2358°	37°/s	PASS
Weak elevator + high damping	15.009%	7.1239 s	40.687 s	-5.2372°	37°/s	PASS
Strong elevator + low damping	17.369%	2.9822 s	20.910 s	-5.1697°	37°/s	PASS
Strong elevator + high damping	16.107%	3.2452 s	21.696 s	-5.1707°	37°/s	PASS

Every tested combined uncertainty case remained stable.

The physical actuator travel constraints were also satisfied in every case, and the imposed $\frac{37^\circ}{s}$ rate limit remained respected.

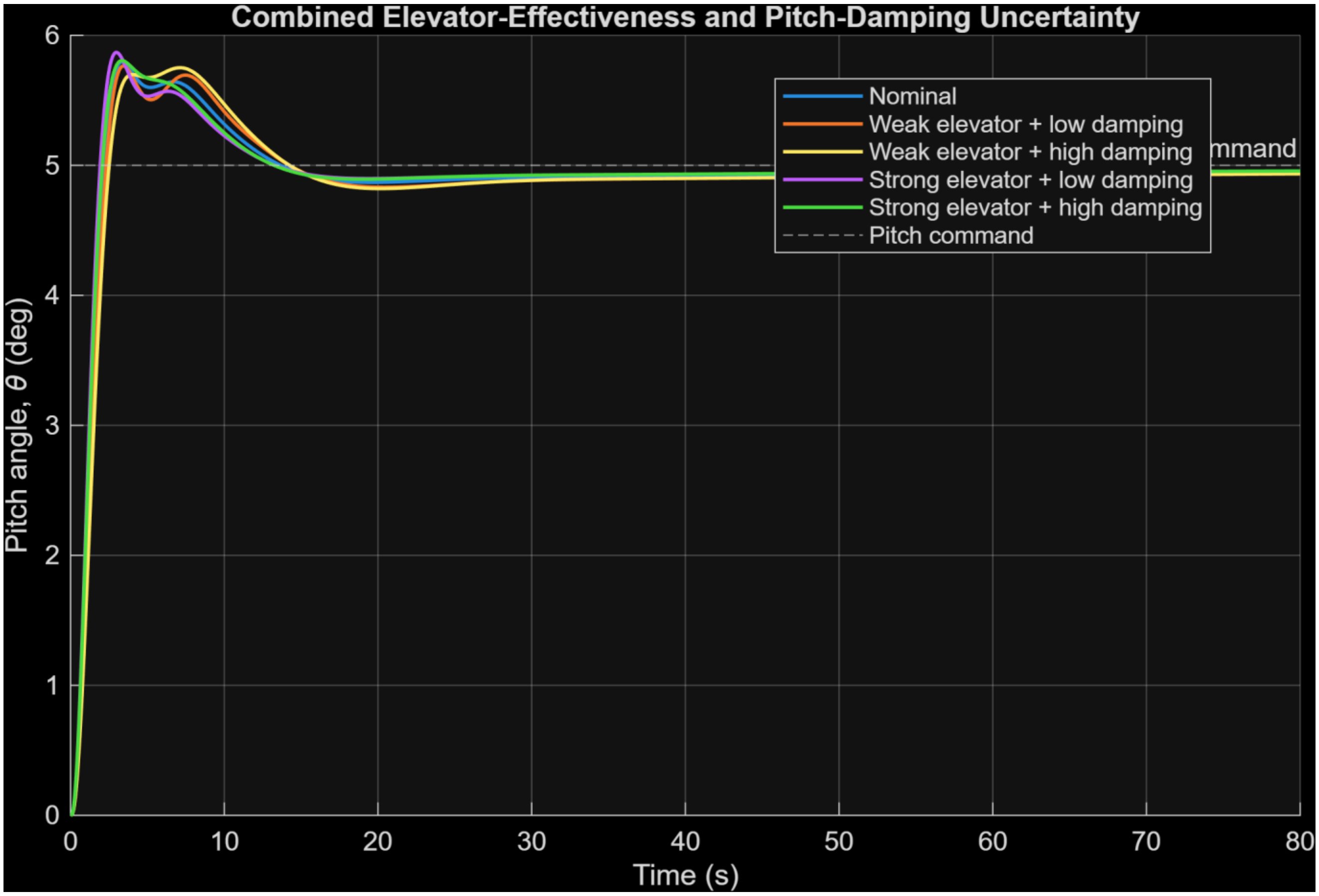

Figure 7. Closed-loop pitch responses for the combined ± 20 elevator-effectiveness and pitch-damping uncertainty corners using the full actuator-constrained model. The weak-elevator cases exhibit the largest settling-time degradation, while all tested cases remain stable and physically feasible.

8.7 Worst-Case Conditions

The largest settling time occurred for the **weak-elevator + low-damping** condition: $t_s = 40.774$ s.

This exceeded the nominal project requirement of $t_s \leq 30$ s.

However, the corresponding overshoot remained only $M_p = 15.285\%$

The largest overshoot occurred under the **strong-elevator + low-damping** condition: $M_p = 17.369\%$

This remained below the 20% project target, while settling time was only $t_s = 20.910$ s.

The worst settling-time condition and the worst overshoot condition therefore occurred at different uncertainty corners.

8.8 Robust Stability and Actuator Feasibility

Across all tested single-parameter and combined uncertainty cases, the aircraft response remained bounded and convergent.

No tested condition produced closed-loop instability.

Therefore, $\boxed{\text{Stable closed-loop behavior was maintained throughout the tested uncertainty set}}$

covering up to $\pm 20\%$

variation in elevator effectiveness and pitch-rate damping.

This should be interpreted as **robustness demonstrated for the specific tested cases**, rather than as a formal mathematical proof of robust stability for every possible aircraft-model variation.

The physical actuator constraints were also satisfied in every full nonlinear uncertainty simulation.

Therefore, $\text{Robust Actuator Feasibility: PASS}$

for the tested uncertainty cases.

8.9 Robust Performance Assessment

The analysis revealed an important distinction between robust stability and robust performance.

The controller remained stable and physically feasible throughout every tested uncertainty case.

However, the nominal transient-performance requirements were not maintained in every case.

The dominant limitation was reduced elevator effectiveness.

In particular, the 20% reduced-effectiveness case produced approximately $t_s = 40.73$ s, which exceeds the 30 s screening criterion.

Pitch-rate-damping uncertainty alone did not cause any performance-screening failure.

The final actuator-aware PID can therefore be summarized as providing robust stability and robust actuator feasibility over the tested cases, but not robust transient-performance compliance across the complete ± 20 elevator-effectiveness range.

8.10 Engineering Interpretation

The sensitivity analysis identified elevator effectiveness as the dominant modeled uncertainty for the final PID architecture.

Reduced elevator effectiveness weakens the relationship between commanded surface motion and the resulting aircraft response.

Integral action still allows the controller to eliminate steady-state pitch error, but the reduced control effectiveness increases the time required for the aircraft to reach the commanded condition.

Pitch-rate-damping uncertainty had considerably less influence over the tested range.

The combined uncertainty study further demonstrated that reduced elevator effectiveness continued to dominate settling-time degradation even when pitch damping was varied simultaneously.

Importantly, this degraded performance was not caused by actuator saturation.

Substantial elevator-travel margin remained available, and the physical actuator constraints continued to be satisfied.

The principal limitation was therefore transient controller performance under reduced aerodynamic control effectiveness rather than inadequate actuator authority.

This result provides a direct motivation for investigating a more capable control architecture in the next stage of the project.

9. Advanced State-Feedback Control

9.1 Objective

The classical PID controller developed in the preceding sections provided stable, physically feasible pitch control, but the robustness study identified a significant performance limitation when elevator effectiveness was reduced.

An advanced state-feedback controller was therefore investigated to determine whether improved transient performance, disturbance rejection, and reduced sensitivity to control-effectiveness changes could be achieved.

Because the Boeing 747 longitudinal aircraft was already represented in state-space form, $\dot{x} = Ax + B_e\delta_e$, Linear Quadratic Regulator (LQR) control was selected as the starting point.

The analysis was subsequently extended to **Linear Quadratic Integral (LQI)** control to provide accurate tracking of nonzero pitch commands.

The final advanced controller was evaluated using the same:

- aircraft model,
- 5° pitch command,
- first-order actuator dynamics,
- elevator travel limits,
- elevator rate limit,
- $+2°$ disturbance,
- 20% reduced-elevator-effectiveness case

used for the final PID evaluation.

9.2 Controllability of the Longitudinal Aircraft

The longitudinal state vector is $x = [u \quad w \quad q \quad \theta]^T$, with elevator deflection δ_e as the single control input.

Before designing a full-state feedback controller, the controllability of the aircraft model was evaluated.

For a four-state system, the controllability matrix is $\mathcal{C}[B_e \quad AB_e \quad A^2B_e \quad A^3B_e]$.

The calculated controllability rank was $\text{rank}(\mathcal{C}) = 4$. Since $\text{rank}(\mathcal{C}) = n$, where $n = 4$, the aircraft is fully controllable through the elevator input at the selected operating condition.

Therefore, Longitudinal Aircraft: Fully Controllable and full-state feedback design is mathematically feasible.

9.3 Initial LQR Design

The LQR controller determines a state-feedback law of the form $\delta_e = -Kx$ by minimizing the quadratic performance index $J = \int_0^\infty (x^T Q x + \delta_e^T R \delta_e)\, dt$.

The matrix (Q) penalizes deviations of the aircraft states, while (R) penalizes control effort.

Rather than selecting arbitrary numerical weights, the initial weighting matrices were constructed using physically interpretable state and actuator normalization scales.

The approximate initial LQR gain was $K = [0.0009 \quad 0.0006 \quad -0.2601 \quad -0.2779]$

The resulting closed-loop poles were approximately $-0.0501 \pm 0.0671i$ and $-0.4736 \pm 0.9211i$.

All poles have negative real parts.

Therefore, Initial LQR Regulation: Stable.

The LQR design successfully stabilized and regulated deviations of the longitudinal states toward zero.

However, regulation about the trim condition is not equivalent to accurate tracking of a nonzero pitch-angle command.

9.4 Static Reference-Prefilter Limitation

To allow the LQR regulator to track the commanded pitch angle, $\theta_{\text{cmd}} = 5°$, a static reference prefilter, N_{bar}, was initially introduced.

The resulting prefilter was approximately $N_{\text{bar}} = -1.9457$.

This produced a command-to-pitch DC gain of unity, meaning that the system had the correct theoretical steady-state tracking gain.

However, the 5° reference step generated an immediate elevator command of approximately $-9.73°$.

The resulting aircraft response reached approximately $\theta_{\max} = 21.51°$, corresponding to approximately 330% overshoot.

The settling time was approximately 118.5 s.

Thus, although the state-feedback system was stable and had correct steady-state gain, stable regulation ≠ satisfactory command tracking.

The static-reference LQR architecture was therefore rejected for the pitch-command problem.

A servo architecture containing integral tracking action was introduced instead.

9.5 LQI Formulation

An integral state was defined from the pitch tracking error: $\dot{\xi}\theta_{\text{cmd}} - \theta$.

The augmented state vector became $\mathbf{x}_a = \begin{bmatrix} \mathbf{x} \\ \xi \end{bmatrix} = \begin{bmatrix} u \\ w \\ q \\ \theta \\ \xi \end{bmatrix}$

The resulting LQI control law was $\delta_e = -K_x\mathbf{x} - K_\xi \xi$.

The augmented state-space system can be written as $\begin{bmatrix} \dot{x} \\ \dot{\xi} \end{bmatrix} = \begin{bmatrix} A & 0 \\ -C_\theta & 0 \end{bmatrix} \begin{bmatrix} x \\ \xi \end{bmatrix} + \begin{bmatrix} B_e \\ 0 \end{bmatrix} \delta_e + \begin{bmatrix} 0 \\ 1 \end{bmatrix} \theta_{cmd}$

The augmented system contains five states.

Its controllability rank was $\text{rank}(\mathcal{C}_a) = 5$.

Therefore, Augmented LQI System: Fully Controllable.

Integral action provides the controller with the ability to generate the sustained elevator bias required for zero steady-state pitch-command error.

9.6 Initial LQI Design

The first LQI design used conservative state, integral-error, and elevator-effort weighting.

The resulting state-feedback gains were approximately $K_x = [-0.0005 \quad 0.0016 \quad -0.4656 \quad -0.6716]$

with integral gain $K_\xi = 0.1$.

The augmented closed-loop poles were approximately -0.0111, $-0.1380 \pm 0.1092i$, and $-0.4964 \pm 0.9380i$.

All poles had negative real parts.

For the nominal $5°$pitch command, the initial LQI design produced approximately 0.67% overshoot and 17.87 s settling time.

When the first-order actuator was included, the maximum actuator rate was only approximately $0.48°/\text{s}$, well below the adopted limit of $37°/\text{s}$.

The initial LQI therefore produced dramatically smoother nominal control action than the actuator-aware PID.

9.7 Long-Duration Equilibrium Validation

The LQI design contains a relatively slow closed-loop mode near -0.0111.

Its corresponding approximate time constant is $\tau \approx \frac{1}{0.0111} \approx 90$ s.

A long-duration simulation was therefore performed to verify the final equilibrium rather than relying only on a shorter transient simulation.

The aircraft DC gain independently predicts that maintaining a $5°$ pitch perturbation requires approximately $\delta_{e,ss} - 5.417°$.

At the end of the extended simulation, the LQI elevator command converged to approximately $-5.416°$, in excellent agreement with the independent equilibrium prediction.

This confirmed that the apparent slow evolution of elevator demand was associated with the slow closed-loop mode rather than with incorrect integral action.

9.8 Initial LQI Limitations

Although the initial LQI produced excellent nominal tracking, additional testing revealed weaknesses that were not apparent from the nominal command response alone.

For the final actuator-aware PID, the tested $+2°$ disturbance produced a disturbance-only pitch peak of $1.2507°$ with recovery in approximately 5.49 s.

The initial conservative LQI produced a larger disturbance response and required approximately 14.26 s to recover.

A second weakness appeared when elevator effectiveness was reduced by 20%.

The initial LQI remained stable and ultimately returned to the commanded pitch, but its settling time increased to approximately 100.9 s.

Long-duration analysis confirmed that the correct equilibrium was still reached.

Therefore, the degraded behavior was caused primarily by **overly conservative controller weighting**, rather than by:

- instability,

- actuator saturation,
- insufficient steady-state control authority.

This result demonstrated that excellent nominal response alone was not sufficient for selecting the final LQI design.

9.9 Structured LQI Weight Tuning

A structured LQI weight study was therefore performed.

The normalization of the physical aircraft states was held fixed while two interpretable design quantities were varied:

- integral-error normalization scale,
- elevator-effort normalization scale.

The integral-error scale was evaluated at 10°s, 7.5°s, 5°s, 2.5°s, while the elevator-effort scale was evaluated at 1°, 1.5°, 2°, 3°.

The combination produced $4 \times 4 = 16$ candidate LQI designs.

Each candidate was evaluated using the same principal engineering tests:

- nominal 5° command tracking,
- 20% reduced elevator effectiveness,
- $+2^\circ$ disturbance rejection,
- actuator-rate demand,
- elevator travel feasibility,
- closed-loop stability.

This changed the LQI design process from tuning for nominal response alone to selecting a controller using **multiple performance and robustness criteria simultaneously**.

9.10 Final Tuned LQI Selection

Two leading candidates from the structured weight study were subsequently evaluated using the complete nonlinear actuator model.

The selected design used the most aggressive tested integral-error weighting together with the least restrictive tested elevator-effort weighting.

The final state-feedback gains, rounded for presentation, were $\boxed{K_x = [-0.0004 \quad 0.0022 \quad -1.6777 \quad -2.6675]}$ with $\boxed{K_\xi = 1.2}$. The final control law is therefore $\boxed{\delta_e = -K_x x - K_\xi \xi}$.

The associated augmented-design poles were approximately -0.0113, -0.3298, -0.5649, and $-0.8863 \pm 1.1879i$.

Every pole has a negative real part. Therefore, Final Tuned LQI: Stable.

9.11 Nonlinear Actuator Validation

The final tuned LQI was evaluated using the same physical actuator model used for the PID: $A(s) = \frac{37}{s+37}$,

with travel limits $-23° \leq \delta_e \leq 17°$ and rate limit $|\dot{\delta}_e| \leq 37°/\text{s}$.

For the nominal 5° pitch command, the tuned LQI produced $\boxed{M_p = 0.6336}$% and $\boxed{t_s = 5.5741 \text{ s}}$.

Maximum actuator rate was only $|\dot{\delta}e|\text{max} = 5.3145°/\text{s}$, well below the physical rate limit.

Under a 20% reduction in elevator effectiveness, the controller produced $M_p = 1.4319\%$ with settling time $t_s = 5.5293$ s and maximum actuator rate of approximately $5.4036°/\text{s}$.

The physical travel and rate limits remained satisfied.

For the+2° disturbance, the tuned LQI limited the disturbance-only pitch excursion to approximately $0.6389°$ and recovered in approximately 4.037 s.

Thus, the final tuned LQI successfully addressed the disturbance and weak-elevator limitations observed with the initial conservative design.

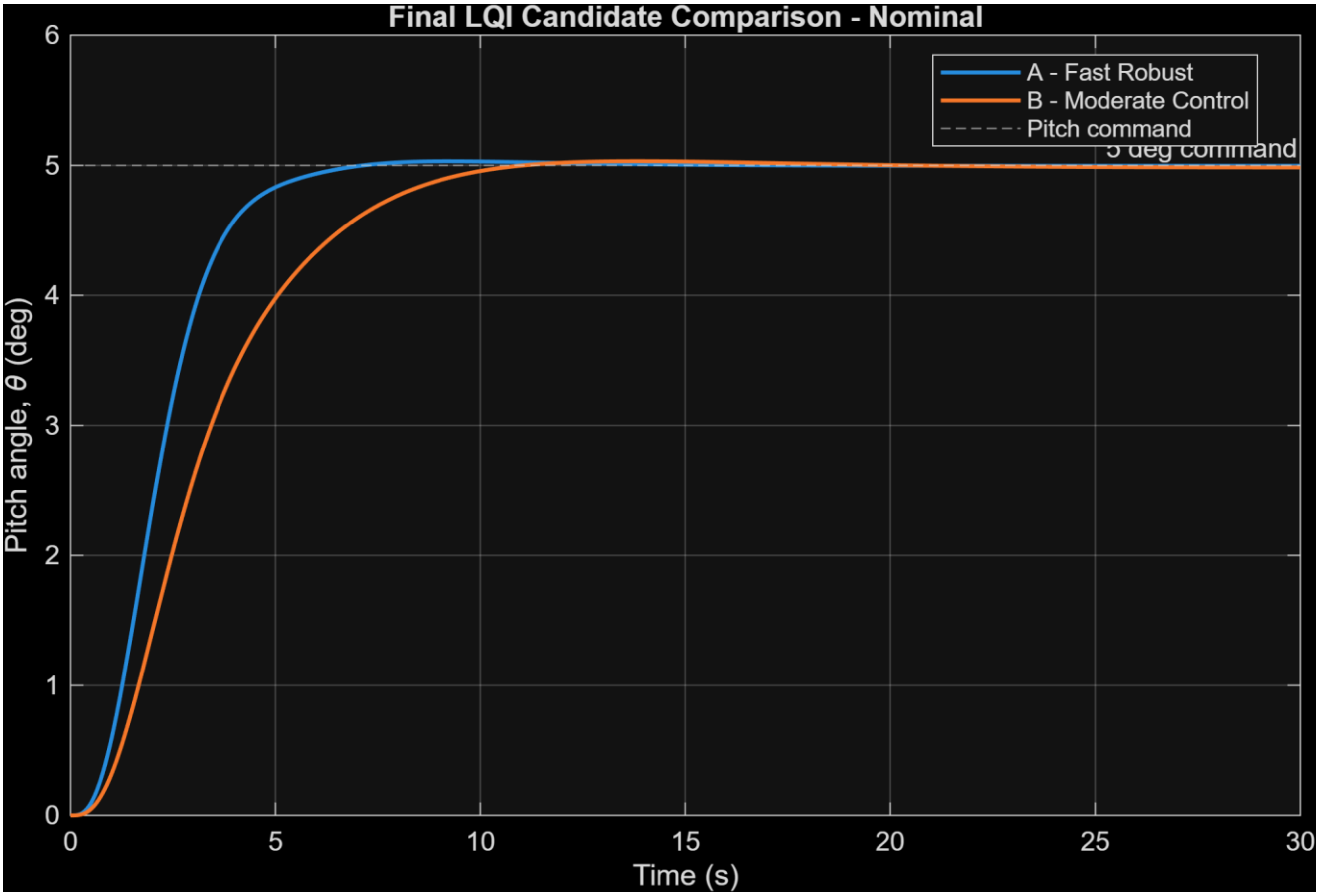

Figure 8. Nominal actuator-constrained response of the final tuned LQI controller to the 5° pitch command, demonstrating rapid command tracking with minimal overshoot.

9.12 Implementation Considerations

The LQI controller provides substantially stronger simulated performance than the classical PID for the cases investigated, but the two architectures have different implementation requirements.

The PID controller primarily relies on measured pitch-angle feedback.

The LQI control law requires the complete longitudinal state vector $x = [u \quad w \quad q \quad \theta]^T$.

Therefore, implementation of the LQI controller would require reliable measurement or estimation of these states.

A practical aircraft implementation could use appropriate sensors together with a state observer or estimator.

However, **no observer or state estimator was designed in this project**.

The LQI results therefore represent the achievable performance of the developed full-state control law under the assumption that the required states are available.

9.13 Engineering Interpretation

The advanced-control study produced several important design conclusions.

First, the conventional LQR regulator was mathematically stable but was not suitable for direct nonzero pitch-command tracking using only a static reference prefilter.

Second, augmenting the controller with integrated pitch error solved the steady-state tracking problem and created an LQI servo controller.

Third, nominal response alone was not sufficient for selecting the LQI weights. The initial conservative LQI produced excellent nominal behavior but performed poorly under disturbance and reduced elevator effectiveness.

A structured multi-case tuning study was therefore required.

The final tuned LQI demonstrated:

- stable closed-loop behavior,
- near-zero nominal overshoot,
- rapid pitch-command tracking,
- low actuator-rate demand,
- strong performance with 20% reduced elevator effectiveness,
- improved rejection of the tested control-channel disturbance,
- compliance with the adopted elevator travel and rate constraints.

The final LQI is therefore carried forward as the **advanced-control candidate** for direct quantitative comparison with the final actuator-aware PID.

10. Final PID versus Tuned-LQI Comparison

10.1 Objective

The final stage of controller comparison evaluated the actuator-aware PID and the tuned LQI using identical aircraft, actuator, command, disturbance, and uncertainty assumptions.

The purpose was not simply to determine which controller produced the fastest nominal response. The comparison considered several engineering criteria simultaneously:

- nominal pitch-command tracking,
- overshoot,
- settling time,
- actuator-rate demand,

- reduced-elevator-effectiveness performance,
- disturbance rejection,
- elevator travel feasibility,
- elevator rate feasibility,
- closed-loop stability,
- implementation complexity.

The final actuator-aware PID was $K_P = 1.0,\ K_I = 0.5,\ K_D = 0.8,\ T_f = 0.1$ s.

The final tuned LQI control law was $\delta_e = -K_x x - K_\xi \xi$, with $K_x = [-0.0004 \quad 0.0022 \quad -1.6777 \quad -2.6675]$, and$K_\xi = 1.2$.

Both controllers were tested using the same actuator model, $A(s) = \frac{37}{s+37}$, with elevator travel limits $-23^\circ \leq \delta_e \leq 17^\circ$ and rate limit $|\dot{\delta}_e| \leq 37^\circ/\mathrm{s}$.

10.2 Final Quantitative Comparison

The principal final results are summarized below.

Table 11. Final PID and Tuned-LQI Performance Comparison

Metric	Final PID	Tuned LQI
Nominal overshoot	15.881%	0.6336%
Nominal 2% settling time	27.074 s	5.5741 s
Nominal maximum actuator rate	37.000°/s	5.3145°/s
20% reduced-effectiveness overshoot	14.328%	1.4319%
20% reduced-effectiveness settling time	40.730 s	5.5293 s
$+2^\circ$disturbance-only pitch peak	1.2507°	0.6389°
$+2^\circ$disturbance recovery time	5.4855 s	4.037 s
Nominal actuator travel	PASS	PASS
Nominal actuator rate	PASS	PASS
Closed-loop stability	PASS	PASS

Both controllers remained stable and physically feasible for the principal validation cases.

However, their transient performance differed substantially.

10.3 Nominal Pitch-Command Tracking

For the nominal $\theta_{\mathrm{cmd}} = 5^\circ$ pitch command, the actuator-aware PID produced $M_{p,\mathrm{PID}} = 15.881\%$ and $t_{s,\mathrm{PID}} = 27.074$ s.

The tuned LQI produced $M_{p,\mathrm{LQI}} = 0.6336\%$ and $t_{s,\mathrm{LQI}} = 5.5741$ s.

The reduction in nominal overshoot was therefore approximately $\frac{15.881-0.6336}{15.881} \times 100 \approx 96.01\%$

The reduction in settling time was approximately $\frac{27.074-5.5741}{27.074} \times 100 \approx 79.41\%$

Thus, the tuned LQI provided a substantially faster and more heavily damped nominal response.

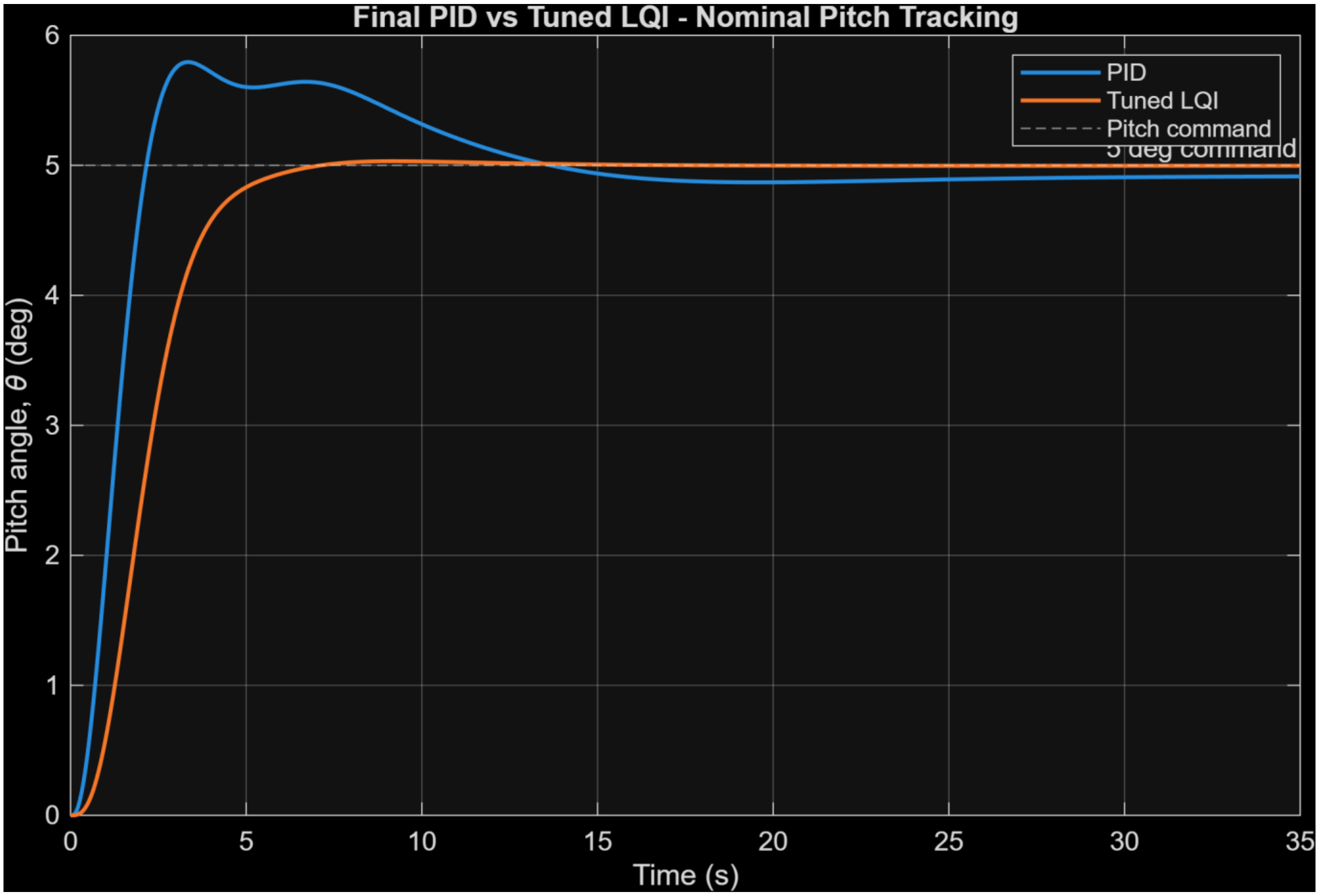

Figure 9. Final actuator-constrained PID and tuned-LQI responses to a (5^\circ) pitch command. The tuned LQI provides substantially lower overshoot and faster settling while both controllers converge to the commanded pitch.

10.4 Actuator-Rate Demand

One of the largest differences between the controllers appeared in actuator-rate demand.

The PID reached the imposed physical rate limit. $37.000°/s$.

The tuned LQI required only $5.3145°/s$.

The corresponding reduction in peak actuator-rate demand was approximately $\frac{37.000-5.3145}{37.000} \times 100 \approx 85.64\%$

The tuned LQI therefore achieved substantially better nominal tracking while using considerably less peak actuator rate.

This is an important result because the improved pitch response was **not obtained by driving the elevator actuator more aggressively**.

Instead, the full-state controller coordinated the longitudinal states more effectively and required substantially less rapid control-surface motion.

10.5 Reduced Elevator Effectiveness

The robustness analysis identified reduced elevator effectiveness as the principal limitation of the final PID.

For a 20% reduction in elevator effectiveness, the PID produced $M_{p,\mathrm{PID}} = 14.328\%$ and $t_{s,\mathrm{PID}} = 40.730$ s.

Although the PID remained stable and physically feasible, its settling time exceeded the project requirement $t_s \leq 30$ s.

The tuned LQI produced $M_{p,\mathrm{LQI}} = 1.4319\%$ and $t_{s,\mathrm{LQI}} = 5.5293$ s.

The LQI settling-time improvement relative to PID was therefore approximately $\frac{40.730-5.5293}{40.730} \times 100 \approx 86.42\%$

The tuned LQI also retained a maximum actuator rate of only approximately $5.4036°/\mathrm{s}$, well below the adopted $37°/\mathrm{s}$ limit.

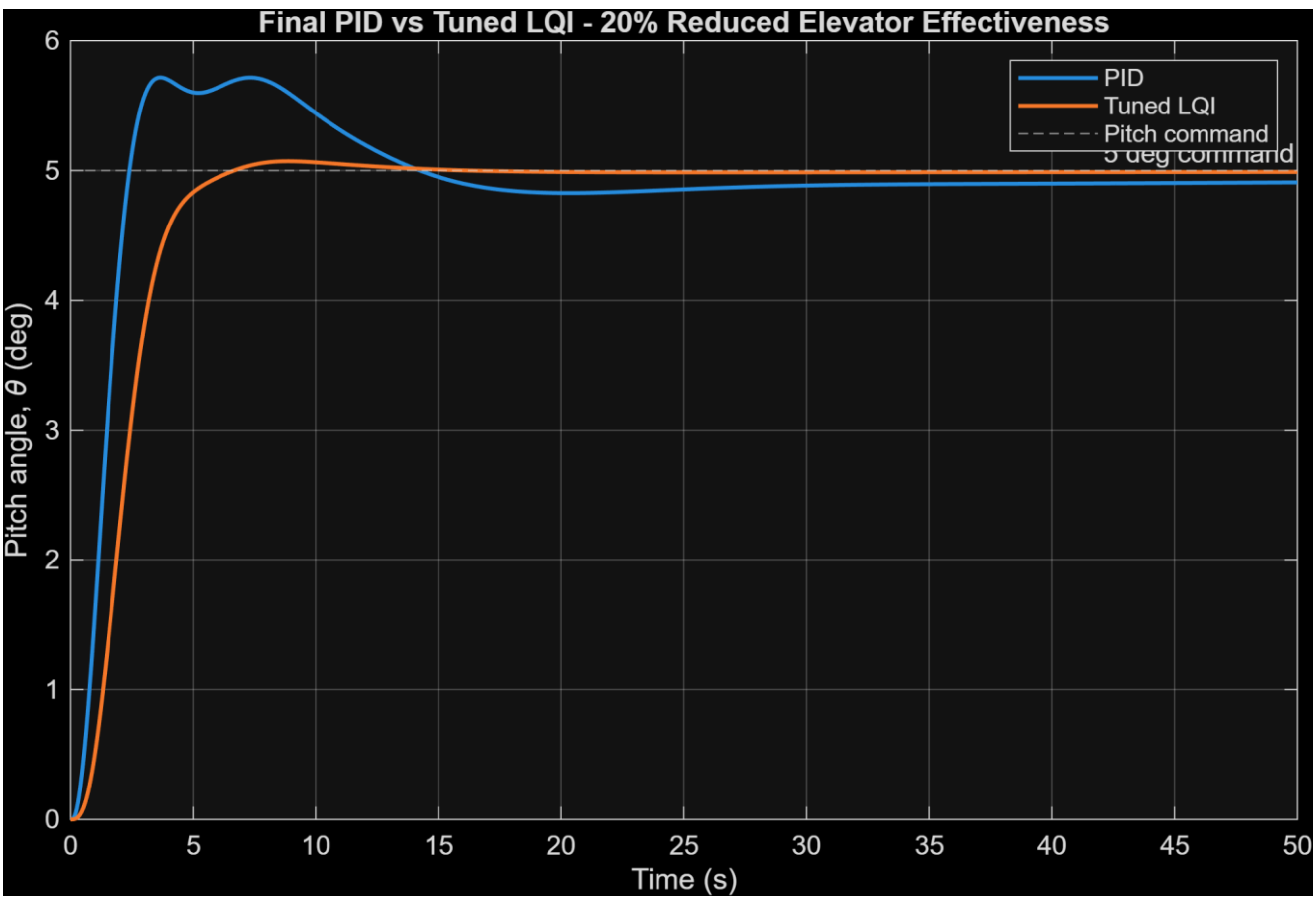

Figure 10. Final PID and tuned-LQI pitch responses with 20% reduced elevator effectiveness. The PID remains stable but exhibits substantially increased settling time, while the tuned LQI maintains rapid command tracking.

10.6 Disturbance-Rejection Comparison

Both controllers were also evaluated using the same additive $+2°$ control-channel disturbance applied from $t = 40$ s to $t = 42$ s. For the final PID, the disturbance-only pitch peak was $|\theta_d|_{\max,\text{PID}} 1.2507°$ with recovery time $t_{\text{rec,PID}} 5.4855$ s.

For the tuned LQI, the disturbance-only pitch peak was reduced to $|\theta_d|_{\max,\text{LQI}} 0.6389°$ with recovery time $t_{\text{rec,LQI}} 4.037$ s.

The disturbance-induced pitch peak was therefore reduced by approximately $\frac{1.2507-0.6389}{1.2507} \times 100 \approx 48.92\%$

The recovery-time reduction was approximately $\frac{5.4855-4.037}{5.4855} \times 100 \approx 26.41$

The tuned LQI therefore limited the disturbance-induced aircraft motion more effectively and returned the aircraft to the commanded pitch more rapidly.

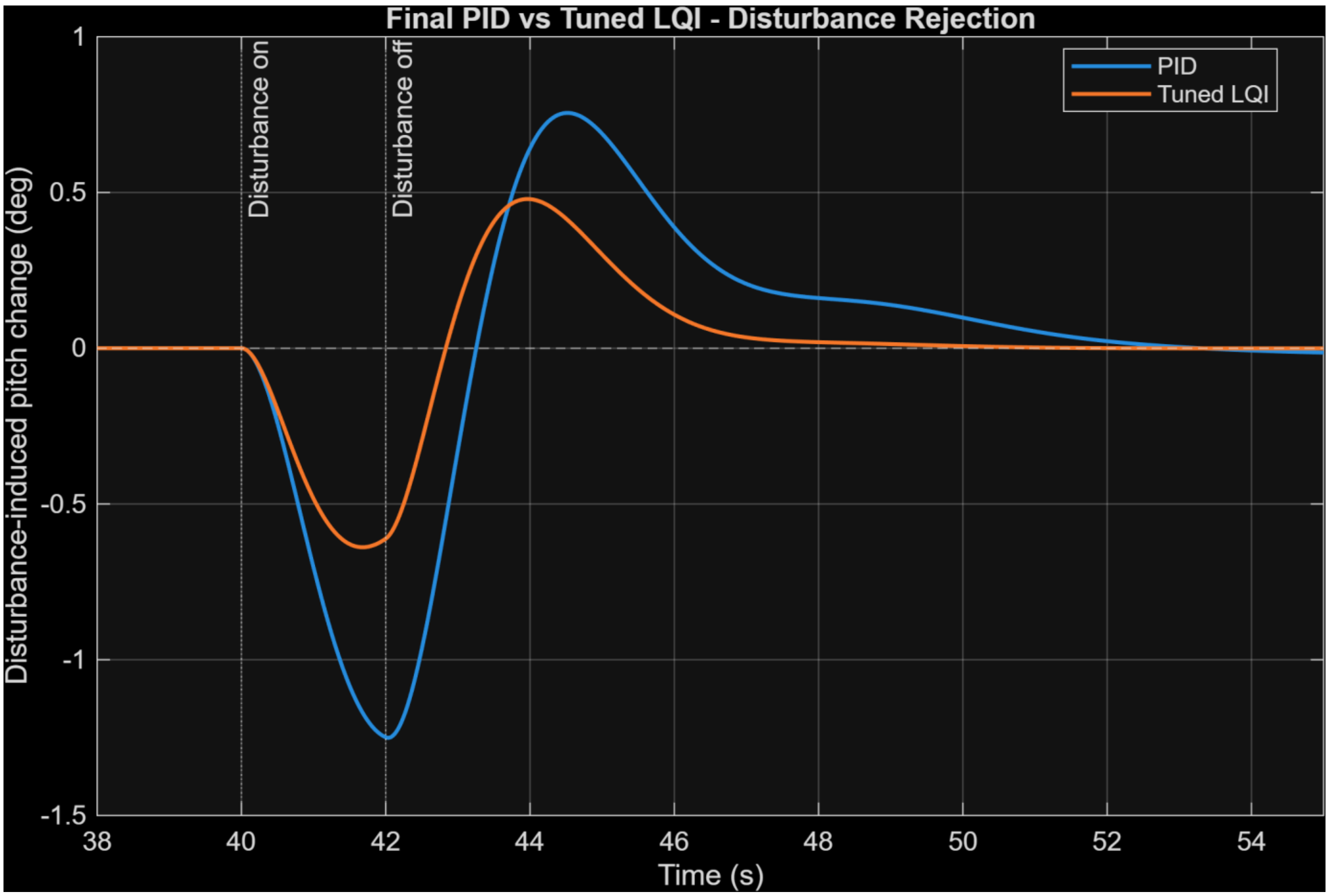

Figure 11. Disturbance-induced pitch response of the final PID and tuned LQI for the $+2°$, 2-second control-channel disturbance. The tuned LQI reduces the disturbance-induced pitch excursion and recovery time.

10.7 Relative Performance Improvements

The principal improvements achieved by the tuned LQI relative to the final actuator-aware PID are summarized below.

Table 12. Relative Performance Improvements with Tuned LQITable 13. Final System Validation Matrix

Performance Quantity	Improvement with Tuned LQI
Nominal overshoot reduction	96.01%
Nominal settling-time reduction	79.41%
Peak nominal actuator-rate reduction	85.64%
Weak-elevator settling-time reduction	86.92%
Disturbance-induced pitch-peak reduction	48.92%
Disturbance recovery-time reduction	26.41%

The tuned LQI therefore improved every principal quantitative performance metric used in the final comparison.

Importantly, these improvements were achieved while maintaining the same aircraft model and the same physical actuator limits.

10.8 Performance-Screening Comparison

The nominal project requirements were $M_p \leq 20\%$ and $t_s \leq 30$ s. The final PID satisfied both requirements under nominal conditions: $15.881\% < 20\%$ and 27.074 s < 30 s.

However, with 20% reduced elevator effectiveness, $t_s = 40.730$ s > 30 s

The PID therefore failed the selected settling-time screening criterion in the weak-elevator case.

The tuned LQI satisfied the requirements under both nominal and reduced-effectiveness conditions: $M_p = 0.6336\%$ for the nominal case, and $M_p = 1.4319\%$ for the weak-elevator case.

Therefore, PID: Nominal Performance PASS but PID: Weak Elevator Performance FAIL whereas Tuned LQI: Nominal and Weak Elevator Performance PASS.

10.9 Classical Simplicity versus Advanced Performance

The quantitative results favor the tuned LQI, but controller selection also involves implementation complexity.

The PID controller has an important practical advantage: it primarily relies on pitch-angle feedback and uses a familiar classical-control architecture.

Its principal strengths are:

- comparatively simple implementation,
- intuitive gain interpretation,
- successful nominal pitch tracking,
- stable disturbance rejection,
- physical actuator feasibility,
- no requirement for the complete state vector.

The tuned LQI uses the full longitudinal state vector, $x = [u \quad w \quad q \quad \theta]^T$, together with the integral state ξ.

Its strengths are:

- substantially lower overshoot,
- much faster settling,
- substantially lower actuator-rate demand,
- improved reduced-effectiveness performance,
- stronger tested disturbance rejection.

However, practical implementation would require reliable measurement or estimation of all required states.

No observer or estimator was developed in the present project.

The comparison therefore represents a trade-off between lower implementation complexity for PID and higher simulated performance for LQI.

10.10 Final Controller Selection

Within the scope of the present simulation study, the tuned LQI is selected as the **highest-performing controller**.

It demonstrated superior performance in every principal quantitative comparison:

- nominal overshoot,
- nominal settling time,
- actuator-rate demand,
- reduced-elevator-effectiveness tracking,
- disturbance-induced pitch deviation,
- disturbance recovery time.

The actuator-aware PID remains an important classical benchmark because it is stable, physically feasible, and considerably simpler to implement.

The final controller hierarchy is therefore Actuator-Aware PIDLower-complexity Classical Benchmark and Tuned LQIHighest-Performing Simulated Controller.

This conclusion is specific to the aircraft model, operating condition, actuator assumptions, uncertainty cases, and disturbance tests investigated in this project.

The final step is therefore to validate both frozen controller configurations independently and confirm that the reported conclusions remain reproducible without further controller tuning.

11. Final System Validation

11.1 Objective

After completion of controller development, actuator modeling, disturbance testing, robustness analysis, and advanced-control tuning, a final independent validation stage was performed.

The purpose of this stage was to verify the completed control system using **frozen controller configurations** rather than continuing to modify controller gains in response to the validation results.

The final validation examined:

- nominal 5° pitch-command tracking,
- 20% reduced elevator effectiveness,
- a $+2°$ additive control-channel disturbance,
- closed-loop stability,
- elevator travel feasibility,
- elevator rate feasibility,
- consistency between final simulations and previously reported results.

No controller gains were modified during this validation stage.

11.2 Frozen Final Configuration

The final classical benchmark was the actuator-aware PID controller $\boxed{K_P = 1.0,\ K_I = 0.5,\ K_D = 0.8,\ T_f = 0.1\ \mathrm{s}}$.

The final advanced controller was the tuned LQI law $\delta_e = -K_x x - K_\xi \xi$ with the presentation gains $\boxed{K_x = [-0.0004 \quad 0.0022 \quad -1.6777 \quad -2.6675]}$ and $\boxed{K_\xi = 1.2}$.

The final actuator model remained $A(s) = \frac{37}{s+37}$, with elevator travel limits $-23° \leq \delta_e \leq 17°$ and maximum actuator rate $|\dot{\delta}_e| \leq 37°/\mathrm{s}$.

The complete frozen controller and actuator configuration was stored as

final_control_configuration.mat.

This file served as the single source of controller parameters for the final validation workflow.

11.3 Final Validation Matrix

Both controllers were evaluated under identical aircraft and actuator assumptions.

The final validation results were:

Controller	Validation Case	Stable	Overshoot	Settling Time	Disturbance Peak	Actuator Limits	Project Performance
PID	Nominal 5°command	PASS	15.881%	27.074 s	—	PASS	PASS
PID	20% reduced elevator effectiveness	PASS	14.328%	40.730 s	—	PASS	FAIL
PID	+2°disturbance	PASS	—	—	1.2507°	PASS	PASS
Tuned LQI	Nominal 5°command	PASS	0.6336%	5.5741 s	—	PASS	PASS
Tuned LQI	20% reduced elevator effectiveness	PASS	1.4319%	5.5293 s	—	PASS	PASS
Tuned LQI	+2°disturbance	PASS	—	—	0.6389°	PASS	PASS

All six final simulated cases remained stable.

All six cases also remained within the adopted elevator travel and rate constraints.

The only project-level performance-screening failure occurred for the PID controller with 20% reduced elevator effectiveness, where $t_s = 40.730$ s exceeded the project criterion $t_s \leq 30$ s.

This independently reproduced the limitation previously identified during the robustness study.

11.4 Preferred-Controller Validation

The tuned LQI passed every principal final validation case.

Under nominal conditions, $M_p = 0.6336\%$ and $t_s = 5.5741$ s. With 20% reduced elevator effectiveness, $M_p = 1.4319\%$ and $t_s = 5.5293$ s.

For the $(+2^\circ)$ disturbance, $|\theta_d|_{\max} = 0.6389^\circ$ with recovery in approximately $t_{\text{rec}} = 4.037$ s.

Maximum nominal LQI actuator rate was only approximately $5.3145^\circ/\text{s}$, substantially below the adopted $37^\circ/\text{s}$ limit. Therefore, Final Tuned LQI Validation: PASS for the nominal command, reduced-elevator-effectiveness, disturbance, stability, actuator-travel, and actuator-rate tests conducted in this project.

11.5 Numerical Consistency Audit

A separate consistency audit was performed to ensure that the values presented throughout the engineering analysis remained consistent with the final frozen simulations.

The audit checked:

- PID nominal overshoot,

- PID nominal settling time,
- PID weak-elevator response,
- PID disturbance response,
- tuned-LQI nominal response,
- tuned-LQI weak-elevator response,
- tuned-LQI disturbance response,
- PID controller gains,
- LQI controller gains,
- actuator dynamics,
- elevator travel limits,
- elevator rate limit.

Previously reported values were compared against the newly generated final results using numerical tolerances appropriate to the displayed rounding precision.

Every comparison remained within the specified tolerance.

The frozen controller configuration also agreed with the controller values documented throughout the report.

Therefore, Final Results Consistency Audit: PASS and Final Configuration consistency Audit: PASS.

This confirms that the final conclusions are reproducible from the frozen system configuration rather than depending on transient MATLAB workspace variables or earlier intermediate controller versions.

11.6 Final Engineering Assessment

The final validation confirms the principal conclusions developed throughout the project.

The actuator-aware PID is a stable and physically feasible classical controller.

Under nominal conditions it satisfies $M_p \leq 20\%$ and $t_s \leq 30$ s, provides effective rejection of the tested control-channel disturbance, and respects the adopted elevator travel and rate constraints.

However, its settling performance degrades significantly when elevator effectiveness is reduced by 20%.

The tuned LQI maintains substantially stronger transient performance under the same reduced-control-authority condition while also requiring considerably less peak actuator rate.

The independently frozen final validation therefore supports the selection Tuned LQI Highest-Performing Controller in the Present Simulation Study.

The actuator-aware PID remains the lower-complexity classical benchmark.

The LQI selection remains subject to the assumption that the complete longitudinal state vector is available for feedback.

12. Conclusions

12.1 Project Summary

This project developed and evaluated a longitudinal pitch-control system for a documented Boeing 747 linearized aircraft model.

The study progressed from aircraft modeling and open-loop analysis through classical feedback design, physical actuator modeling, disturbance rejection, robustness assessment, advanced full-state control, and independent final validation.

The baseline aircraft was modeled using the longitudinal state vector $x = [u \quad w \quad q \quad \theta]^T$ with elevator deflection δ_e as the control input and pitch angle θ as the principal-controlled output.

The aircraft model was reconstructed from documented source data and independently checked against the published state-space representation before being frozen for subsequent analysis.

12.2 Open-Loop Aircraft Dynamics

The open-loop Boeing 747 model was asymptotically stable at the selected cruise operating condition.

The longitudinal dynamics contained a short-period mode with poles approximately $-0.3717 \pm 0.8869i$ and a lightly damped phugoid mode with poles approximately $-0.0033 \pm 0.0672i$.

The short-period damping ratio was approximately $\zeta_{SP} = 0.3865$, while the phugoid damping ratio was only $\zeta_{PH} = 0.0489$.

The resulting open-loop response required approximately 1712 s to satisfy the selected 2% settling criterion.

The analysis therefore demonstrated that open-loop stability does not imply satisfactory pitch-control performance.

12.3 Classical Controller Development

P, PI, and PID controllers were developed sequentially.

Proportional feedback improved the aircraft response but retained a steady-state tracking error of approximately $1.7568°$.

Integral feedback eliminated the steady-state error but retained significant overshoot and relatively slow settling.

A filtered PID controller produced the strongest classical response.

After realistic actuator constraints were introduced, the controller was reassessed and the final actuator-aware PID became $K_P = 1.0,\ K_I = 0.5,\ K_D = 0.8,\ T_f = 0.1$ s. Its nominal performance was $M_p = 15.881\%$ and $t_s = 27.074$ s.

Thus, the final PID satisfied the nominal project performance targets.

12.4 Importance of Actuator Modeling

Introducing physical actuator behavior produced one of the most important findings of the project.

The first-order actuator lag, $A(s) = \frac{37}{s+37}$, changed the nominal pitch response only slightly.

However, examination of elevator motion showed that the unconstrained actuator would require an initial rate of approximately $148°/\mathrm{s}$, four times the adopted physical limit of $37°/\mathrm{s}$.

The complete actuator model therefore included both rate and travel constraints: $|\dot{\delta}_e| \leq 37°/\mathrm{s},\ -23° \leq \delta_e \leq 17°$.

The controller selected using the ideal actuator slightly violated the project overshoot target after the physical rate limit was introduced.

This required an actuator-aware controller reassessment.

The project therefore demonstrated that actuator feasibility must be evaluated directly rather than inferred from aircraft response alone.

12.5 Disturbance-Rejection Result

The final actuator-aware PID was subjected to additive elevator/control-channel disturbances.

For the final $+2°$ disturbance, the disturbance-only pitch response reached $1.2507°$ and returned to within $\pm 0.1°$ of the commanded condition in approximately 5.4855 s.

The tested disturbance-rejection maneuver remained within the modeled actuator limits.

The final tuned LQI improved these values to $0.6389°$ disturbance-induced pitch excursion and approximately 4.037 s recovery time.

12.6 Robustness Result

The final PID was evaluated under up to $\pm 20\%$ changes in elevator effectiveness and pitch-rate damping.

All tested uncertainty cases remained stable.

The actuator travel and rate constraints also remained satisfied in every full nonlinear uncertainty simulation.

Pitch-rate-damping variation had comparatively little effect on the closed-loop response.

Reduced elevator effectiveness was the dominant modeled uncertainty.

With 20% reduced elevator effectiveness, the final PID settling time increased to 40.730 s, causing failure of the project's 30 s settling-time target despite continued stability and actuator feasibility.

The robustness analysis therefore demonstrated a distinction between robust stability and robust performance.

12.7 Advanced-Control Result

A conventional LQR controller was first developed and verified as a stable regulator.

However, static-prefilter tracking of a nonzero pitch command produced unacceptable transient behavior.

Integral pitch-error feedback was therefore introduced to form an LQI servo controller.

An initial conservative LQI achieved strong nominal performance but displayed poor disturbance response and slow weak-elevator adaptation.

A structured 16-candidate weighting study was then conducted using nominal tracking, reduced elevator effectiveness, disturbance rejection, and actuator demand as simultaneous design criteria.

The final tuned LQI was $\delta_e = -K_x x - K_\xi \xi$ with $K_x = [-0.0004 \quad 0.0022 \quad -1.6777 \quad -2.6675]$ and $K_\xi = 1.2$.

The final LQI achieved 0.6336% nominal overshoot, 5.5741 s nominal settling time, and peak actuator rate of only $5.3145°/\text{s}$.

12.8 Final PID–LQI Result

Relative to the actuator-aware PID, the tuned LQI reduced:

- nominal overshoot by approximately **96.01%**,
- nominal settling time by approximately **79.41%**,
- nominal peak actuator rate by approximately **85.64%**,
- weak-elevator settling time by approximately **86.42%**,
- disturbance-induced pitch peak by approximately **48.92%**,
- disturbance recovery time by approximately **26.41%**.

The tuned LQI therefore provided the strongest simulated performance of all controller architectures investigated.

The PID remains attractive because of its lower implementation complexity, while LQI offers substantially stronger simulated performance when full-state feedback is available.

12.9 Final Conclusion

The completed project demonstrates a full control-system engineering progression:

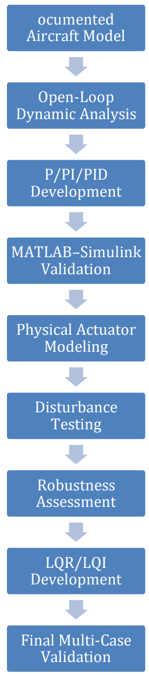

The principal engineering conclusion is that progressively increasing model realism changed the controller-design decisions.

A controller that appeared satisfactory with an ideal actuator required reassessment after the actuator-rate limitation was introduced.

Similarly, a controller that performed well under nominal conditions required additional testing before its robustness could be judged.

The final tuned LQI provided the strongest overall simulated response, while the actuator-aware PID remained a stable and feasible lower-complexity benchmark.

The final numerical consistency audit confirmed that these conclusions were reproducible using the frozen aircraft and controller configurations.

13. Limitations and Future Work

13.1 Linear Aircraft Model

The aircraft model used in this study is a linear small-perturbation representation developed about one specific cruise operating condition.

Consequently, the results apply locally around the selected trim point and should not automatically be extended to the complete Boeing 747 flight envelope.

The model does not explicitly represent:

- stall,
- large-angle maneuvers,
- strongly nonlinear aerodynamic behavior,
- large changes in Mach number,
- large changes in altitude,
- nonlinear control-surface effectiveness.

The controller results should therefore be interpreted as a longitudinal control study near the modeled trim condition.

13.2 Longitudinal Dynamics Only

Only longitudinal aircraft motion was considered.

The modeled states were $\mathbf{x}_{long} = [u \quad w \quad q \quad \theta]^T$ Lateral-directional dynamics such as $\mathbf{x}_{lat-dir} = [v \quad p \quad r \quad \phi \quad \psi]^T$ were outside the scope of the project.

Coupling between longitudinal and lateral-directional aircraft motion was therefore not evaluated.

A future extension could employ a complete six-degree-of-freedom aircraft model.

13.3 Rigid-Aircraft Assumption

The aircraft was treated as a rigid body.

Structural flexibility and aeroelastic effects were not included in the flight-control model.

Consequently, interactions between the pitch-control system and flexible structural modes were not evaluated.

For a higher-fidelity study, flexible-body dynamics could be included before evaluating controller bandwidth and stability margins.

13.4 Actuator-Model Limitation

The baseline longitudinal dynamics and actuator constraints were obtained from separate documented Boeing 747 sources.

The actuator model was adopted as a representative B747-100/200 actuator benchmark: $A(s) = \frac{37}{s+37}$, with travel limits $-23° \leq \delta_e \leq 17°$ and rate limit $|\dot{\delta}_e| \leq 37°/\text{s}$.

The project does not claim that the baseline aircraft state-space model and the actuator source represent the exact same Boeing 747 configuration, loading condition, or trim point.

A future study could use a fully configuration-matched aircraft and actuator dataset.

13.5 Uncertainty-Study Limitation

The $\pm 20\%$ elevator-effectiveness and pitch-damping variations were selected as engineering sensitivity cases.

They are **not certified Boeing 747 uncertainty bounds**.

The sensitivity analysis therefore demonstrates controller behavior over the tested parameter variations rather than providing a formal proof of robust stability over a rigorously defined uncertainty set.

Future analysis could use:

- experimentally justified uncertainty bounds,
- Monte Carlo simulation,
- structured singular-value analysis,
- probabilistic parameter distributions,
- formal robust-control methods.

13.6 Disturbance-Model Limitation

The disturbance model used in this study was an additive control-channel disturbance.

It provided a controlled method for comparing feedback disturbance rejection, but it does not represent the complete physical disturbance environment of an aircraft.

The simulations did not explicitly model:

- atmospheric turbulence,
- vertical gusts,
- wind shear,
- sensor disturbances,
- structural excitation,
- engine disturbances.

Future work could introduce aerodynamic gust and turbulence models directly into the aircraft force and moment equations.

13.7 Full-State Feedback Assumption

The tuned LQI controller assumes availability of the complete longitudinal state vector: $x = [u \quad w \quad q \quad \theta]^T$.

No state observer or estimator was developed in the present project.

A practical implementation would therefore require appropriate sensors and/or estimated states.

A logical next extension would be development of a state observer, such as:

- a Luenberger observer,
- a Kalman filter,
- another suitable state-estimation architecture.

The resulting controller-estimator combination could then be tested with sensor noise and model uncertainty.

13.8 Sensor and Computational Effects

The final simulations did not include a detailed model of:

- sensor noise,
- sensor bias,
- sensor bandwidth,
- data-sampling effects,
- computational delay,
- communication delay,
- digital controller discretization.

These effects can influence practical flight-control performance, particularly for higher-bandwidth state-feedback controllers.

Future work should therefore evaluate the tuned LQI after introducing realistic measurement and implementation effects.

13.9 Gain Scheduling and Flight-Envelope Extension

The controller gains were designed for one operating condition.

An aircraft operating over a broad range of altitude, speed, mass, and center-of-gravity conditions will experience changing dynamics.

A more complete flight-control architecture could therefore develop controllers at multiple trim conditions and interpolate between them using gain scheduling.

This would allow the control law to address a broader portion of the aircraft flight envelope.

13.10 Nonlinear and Six-Degree-of-Freedom Validation

A major future development would be migration from the current linear longitudinal plant to a nonlinear six-degree-of-freedom simulation.

The current controller could then be tested under:

- larger pitch commands,
- simultaneous longitudinal and lateral motion,
- nonlinear aerodynamic coefficients,
- changing airspeed and altitude,
- larger disturbance amplitudes,
- more realistic atmospheric conditions.

This would provide a stronger bridge between the present control-design study and a high-fidelity aircraft simulation.

13.11 Hardware-in-the-Loop and Experimental Validation

The present project is simulation-based.

No hardware-in-the-loop or flight-test validation was performed.

A future implementation could deploy the control algorithm on real-time hardware and connect it to a real-time aircraft simulation.

Such testing could evaluate:

- sampling effects,
- computational latency,
- actuator-command interfaces,
- sensor interfaces,
- numerical execution time,
- controller behavior under real-time constraints.

Hardware-in-the-loop testing would provide a practical intermediate step between desktop simulation and physical flight testing.

13.12 Recommended Future Development Path

A logical continuation of the project would be:

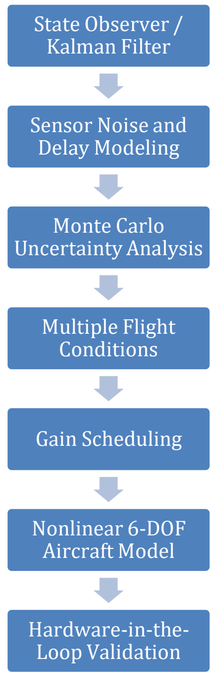

These extensions were **not completed in the present project** and are proposed only as future development opportunities.

References

[1] J. P. How, "Aircraft Longitudinal Dynamics," Lecture 6, *16.333 Aircraft Stability and Control*, Massachusetts Institute of Technology OpenCourseWare, Cambridge, MA, USA, Fall 2004.

[2] J. P. How, "Basic Longitudinal Control," Lecture 9, *16.333 Aircraft Stability and Control*, Massachusetts Institute of Technology OpenCourseWare, Cambridge, MA, USA, Fall 2004.

[3] R. K. Heffley and W. F. Jewell, *Aircraft Handling Qualities Data*, NASA CR-2144, Systems Technology, Inc., Hawthorne, CA, USA, 1972.

[4] J. Y. Shin, "Robust Gain-Scheduled Fault Tolerant Control for a Transport Aircraft," NASA Technical Reports Server, Document ID 20070032920, 2007.

[5] The MathWorks, Inc., *MATLAB Documentation*, Natick, MA, USA.

[6] The MathWorks, Inc., *Simulink Documentation*, Natick, MA, USA.

[7] The MathWorks, Inc., *Control System Toolbox Documentation*, Natick, MA, USA.

Appendices

Appendix A — Baseline Aircraft Model

The frozen longitudinal aircraft model uses $x = [u \quad w \quad q \quad \theta]^T$ and elevator deflection δ_e as the control input.

The state-space representation is $\dot{x} = Ax + B_e\delta_e$ with $A \approx \begin{matrix} -0.0069 & 0.0139 & 0 & -9.81 \\ -0.0905 & -0.3149 & 235.8928 & 0 \\ 0.0004 & -0.0034 & -0.4282 & 0 \\ 0 & 0 & 1 & 0 \end{matrix}$ and $B_e \approx$

$$\begin{matrix} -5.726 \times 10\text{^}(-5) \\ -5.508 \\ -1.157 \\ 0 \end{matrix}$$

Pitch angle is extracted using $C_\theta = [0 \quad 0 \quad 0 \quad 1]$, with $D_\theta = 0$.

The validated baseline plant is stored as

B747_longitudinal_baseline.mat.

Appendix B — Final Controller and Actuator Configuration

B.1 Final Actuator-Aware PID

$$K_P = 1.0, \qquad K_I = 0.5, \qquad K_D = 0.8, \qquad T_f = 0.1\ \text{s}$$

B.2 Final Tuned LQI

$$\boldsymbol{\delta_e = -K_x x - K_\xi \xi}$$

with

$$K_x \approx [-0.0004 \quad 0.0022 \quad -1.6777 \quad -2.6675]$$

and

$$K_\xi = 1.2$$

.

B.3 Final Actuator Model

$$A(s) = \frac{37}{s + 37}$$

$$-23^\circ \le \delta_e \le 17^\circ$$

$$|\dot{\delta}_e| \le 37^\circ/\text{s}.$$

The frozen final configuration is stored as

final_control_configuration.mat.

Appendix C — Key MATLAB and Simulink Files

The principal project files used in the final engineering analysis include:

Aircraft Modeling and Open-Loop Analysis

- phase4_b747_model.m
- phase5_open_loop_modes.m
- phase5_open_loop_response.m
- phase6_matlab_simulink_validation.m
- phase6_b747_baseline.slx

Classical Controller Development

- phase7_p_final.m
- phase7_pi_final.m
- phase7_pid_final.m
- phase7_controller_comparison.m
- phase7_pid_matlab_simulink_validation.m
- phase7_b747_pid_closed_loop.slx

Actuator and Disturbance Analysis

- phase10_actuator_dynamics.m
- phase10_actuator_limit_check.m
- phase10_constrained_controller_comparison.m
- phase10_final_constrained_controller.m
- phase10_constrained_disturbance_2deg.m
- phase10_b747_actuator_limits.slx

Robustness Analysis

- phase11_elevator_effectiveness_sensitivity.m
- phase11_weak_elevator_constrained.m

- phase11_pitch_damping_sensitivity.m
- phase11_combined_uncertainty.m

Advanced Controller Development

- phase12_lqr_controllability.m
- phase12_lqr_initial_design.m
- phase12_lqi_initial_design.m
- phase12_lqi_weight_grid.m
- phase12_lqi_final_candidate_validation.m
- phase12_final_pid_lqi_comparison.m
- phase12_b747_lqi_actuator_limits.slx

Final Validation

- phase13_freeze_final_configuration.m
- phase13_master_validation.m
- phase13_consistency_audit.m

Appendix D — Numerical Consistency Audit

A final numerical consistency audit was performed after freezing the aircraft, controller, and actuator configurations. The purpose of the audit was to verify that the quantitative results reported throughout the document remained consistent with values regenerated from the final simulation configuration.

Reported quantities were compared with the independently regenerated results using numerical tolerances selected to be smaller than the displayed rounding precision. All audited quantities remained within their specified tolerances.

D.1 Final-Results Consistency Audit

Table 14. Final Results Consistency Audit

Quantity	Reported Value	Absolute Difference	Tolerance	Result
PID nominal overshoot	15.881%	0.00031472%	0.001%	PASS
PID nominal settling time	27.074 s	0.00027012 s	0.001 s	PASS
PID -20% elevator-effectiveness overshoot	14.328%	0.00020613%	0.001%	PASS

PID -20% elevator-effectiveness settling time	40.730 s	0.000259498	0.001 s	PASS
PID disturbance-only pitch peak	1.2507°	$(7.4009 \times 10^{-6})°$	0.0001°	PASS
PID disturbance recovery time	5.4855 s	$(9.0012 \times 10^{-7})s$	0.0001 s	PASS
Tuned-LQI nominal overshoot	0.63364%	$(4.9713 \times 10^{-6})\%$	0.001%	PASS
Tuned-LQI nominal settling time	5.5741 s	$(3.5616 \times 10^{-5})°/s$	0.001 s	PASS
Tuned-LQI nominal peak actuator rate	5.3145°/s	$(4.5871 \times 10^{-5})\%$	0.001°/s	PASS
Tuned-LQI −20% elevator-effectiveness overshoot	1.4319%	$(3.9049 \times 10^{-5})s$	0.001%	PASS
Tuned-LQI −20% elevator-effectiveness settling time	5.5293 s	$(4.3751 \times 10^{-5})°/s$	0.001 s	PASS
Tuned-LQI −20% elevator-effectiveness peak actuator rate	5.4036°/s	$(1.2751 \times 10^{-6})°$	0.001°/s	PASS
Tuned-LQI disturbance-only pitch peak	0.6389°	$(4.4311 \times 10^{-5})s$	0.0001°	PASS
Tuned-LQI disturbance recovery time	4.0370 s		0.0001 s	PASS

Final Results Consistency Audit: PASS

Every audited response quantity reproduced the previously reported value to within the adopted numerical tolerance. The small differences are substantially below the precision used for presentation in the main report and are attributable to numerical rounding and simulation output precision.

D.2 Final-Configuration Consistency Audit

The frozen controller and actuator parameters were also checked independently against the values documented in the report.

Table 15. Final Controller and Actuator Configuration Audit

Parameter	Documented Value	Frozen Configuration	Result
PID (K_p)	1.0	1.0	PASS
PID (K_i)	0.5	0.5	PASS
PID (K_d)	0.8	0.8	PASS
PID derivative-filter time constant (T_f)	0.1 s	0.1 s	PASS

LQI (K_u)	-0.0004	−0.0004253	PASS
LQI (K_w)	0.0022	0.0022330	PASS
LQI (K_q)	-1.6777	approximately −1.6777	PASS
LQI (K_θ)	-2.6675	approximately −2.6675	PASS
LQI(K_ξ)	1.2	1.2	PASS
Actuator pole	37 rad/s	37 rad/s	PASS
Elevator lower travel limit	−23°	−23°	PASS
Elevator upper travel limit	+17°	+17°	PASS
Elevator rate limit	37°/s	37°/s	PASS

The small differences between the rounded LQI gains reported in the main document and the stored controller values arise solely from presentation rounding. The simulations used the full-precision gains stored in the frozen final configuration.

Final Configuration Consistency Audit: PASS

The combined audit confirms that the final numerical conclusions can be reproduced from the frozen project configuration and are not dependent on intermediate controller versions or transient MATLAB workspace variables.